Evolutionary analysis of the exocyst complex in streptophytes links early EXO70 diversification with dominance over SEC3 in membrane targeting

Samuel Haluška[a,b†], Edita Janková-Drdová[a,†], Matěj Drs[a,b], George Alexandru Caldarescu[b,c], Roman Skokan[a], Přemysl Pejchar[a], Viktor Žárský[a,b] and Martin Potocký[a]*

[a] Institute of Experimental Botany, Czech Academy of Sciences, Rozvojová 263, 165 02 Prague, Czech Republic

[b] Department of Experimental Plant Biology, Faculty of Science, Charles University, Viničná 5, 128 44 Prague, Czech Republic

[c] Current address – Max Planck Institute for Plant Breeding Research, Carl-von-Linne-Weg 10 D-50829 Cologne, Germany

† This authors contributed equally to the work

* Author for correspondence: Martin Potocký (potocky@ueb.cas.cz)

Short title: **EXO70-driven evolution of the plant exocyst**

ABSTRACT

The exocyst is an evolutionarily conserved vesicle-tethering complex composed of two modules (I: SEC3, SEC5, SEC6, SEC8; II: SEC10, SEC15, EXO70, EXO84). In plants, the module II subunits SEC15, EXO84, and particularly EXO70 have diversified into distinct subfamilies, yet the evolutionary origins and functional consequences of this diversification remain unclear. Here, we reconstruct the evolutionary history of the exocyst across streptophytes and combine phylogenetic analyses with cross-species functional complementation and structural modeling to investigate how exocyst membrane targeting evolved. We show that the three major EXO70 subfamilies emerged already in anydrophytes—the common ancestor of Zygnematophyceae and Embryophyta—and subsequently expanded independently in multiple lineages. Complementation experiments using the liverwort *Marchantia polymorpha* and the streptophyte alga *Klebsormidium nitens* demonstrate that canonical EXO70 function is deeply conserved and retained in the EXO70.1 lineage, whereas other subfamilies exhibit pronounced functional specialization. Importantly, we uncover an evolutionary shift in exocyst membrane targeting: whereas Klebsormidium SEC3 retains autonomous exocyst membrane-recruitment capacity, land-plant SEC3 subunits have lost this ability, rendering exocyst membrane targeting increasingly dependent on EXO70. We propose that this shift, together with early EXO70 diversification, enabled paralog-specific exocyst targeting and facilitated the evolution of specialized secretion pathways during plant terrestrialization.

KEYWORDS

Exocyst complex, evolution, phylogeny, EXO70, SEC3, plasma membrane, exocytosis, Streptophyta, Klebsormidium, Marchantia, Arabidopsis

INTRODUCTION

The exocyst complex is an evolutionarily conserved, hetero-octameric tethering complex that directs secretory vesicles to the plasma membrane (PM) prior to SNARE-mediated membrane fusion (TerBush *et al*., 1996; He and Guo, 2009; Heider *et al*., 2016). Composed of eight subunits—SEC3, SEC5, SEC6, SEC8, SEC10, SEC15, EXO84, and EXO70—the exocyst is organized into two structural and functional modules: module I (SEC3, SEC5, SEC6, SEC8) and module II (SEC10, SEC15, EXO84, EXO70), which assemble via N-terminal CorEX helical bundles (Koumandou *et al*., 2007; Mei *et al*., 2018; Synek *et al*., 2021). While this modular exocyst architecture, dating to the last eukaryotic common ancestor, is preserved across diverse lineages, the contributions of individual subunits to complex function, their evolutionary diversification, and their functional conservation in plants remain largely unresolved.

In plants, the exocyst is essential for polarized growth, cell morphogenesis, and cytokinesis (Hála *et al*., 2008; Drdová *et al*., 2013; Fendrych *et al*., 2013; Žárský *et al*., 2013; Vukašinović *et al*., 2017), and has also been implicated in autophagy-related processes (Kulich *et al*., 2013; Žárský, 2022). In the model angiosperm *Arabidopsis thaliana*, multiple exocyst subunits accumulate at sites of intense secretion, including the forming cell plate during cytokinesis, where SEC6, SEC8, SEC15b, EXO70A1, and EXO84B exhibit distinct temporal and spatial accumulation patterns (Fendrych *et al*., 2010). Exocyst subunits also co-localize as discrete foci at exocytically active plasma membrane domains in growing root epidermal cells (Fendrych *et al*., 2013). Genetic disruption of core exocyst subunits, including SEC3, SEC6, SEC8, SEC15, or EXO84, results in severe developmental defects, underscoring the conserved requirement for an intact exocyst complex in plant growth and viability (Synek *et al*., 2006; Kulich *et al*., 2010).

While exocyst subunits are encoded by a single gene in yeast or by a few paralogs in metazoans, the land plant exocyst exhibits a striking feature: expansion of the EXO70 family to 23 paralogs in Arabidopsis and 47 paralogs in rice (Eliáš *et al.,* 2003; Synek *et al*., 2006; Chong *et al.,* 2010; Cvrčková *et al*., 2012). Previous phylogenetic analyses have identified three major land-plant EXO70 clades, proposed to have emerged around the divergence of charophyte algae and land plant (embryophyte) lineages (Cvrčková *et al.,* 2012; Žárský *et al.*, 2020). In contrast, other angiosperm exocyst subunits (except EXO84) are encoded by three or fewer paralogs (Cvrčková *et al*., 2012). Among Arabidopsis EXO70 paralogs, the EXO70A clade (belonging to the EXO70.1 subfamily) has been the most extensively studied due to its near-ubiquitous expression pattern and the severe phenotypic deviations of *exo70A1* loss-of-function mutants. These include dwarfism, loss of apical dominance, disruption of polarized cell expansion in root hairs, and near-complete sterility (Synek *et al.,* 2006; Kulich *et al*., 2010). Another EXO70 isoform, EXO70B1, is implicated in autophagy: loss-of-function mutants show reduced vacuole anthocyanin accumulation and spontaneous hypersensitive response-like lesions on leaves (Kulich *et al.,* 2013). Isoform EXO70H4 is involved in Arabidopsis trichome secondary cell wall biogenesis by delivering callose to a specific plasma membrane—cell wall domain (Kulich *et al*., 2015; Kulich *et al*., 2018).

A key mechanistic feature of the exocyst is that its membrane targeting—the process by which the complex is recruited to specific PM domains—strongly depends on interactions between specific subunits and negatively charged phospholipids. In yeast and mammals, both EXO70 and SEC3 serve as membrane-targeting landmarks through their phosphoinositide-binding surfaces (Boyd *et al*., 2004; Wu *et al*., 2008; Zhang *et al*., 2008; Pleskot *et al*., 2015; Maib and Murray, 2022). These interactions position the exocyst at sites of polarized secretion, enabling small GTPase-regulated vesicle delivery

and localized cell expansion (He *et al*., 2007; He and Guo, 2009; Heider and Munson, 2012). Importantly, the electrostatic properties of protein surfaces determine the affinity and specificity of membrane association. Because membrane-binding surfaces are also often involved in protein–protein interactions within the exocyst core, electrostatic properties represent an evolutionarily tunable parameter that can simultaneously influence membrane targeting and inter-subunit interfaces (Zhou and Pang, 2018; De La Concepción *et al*., 2025).

In angiosperms, the balance between EXO70 and SEC3 in membrane targeting differs markedly from the yeast paradigm. Although Arabidopsis SEC3 retains a lipid-binding PH domain, its contribution to exocyst PM localization is minor (Bloch et al., 2016); instead, EXO70A1 dominates exocyst membrane recruitment in the Arabidopsis sporophyte (Synek et al., 2021). Similarly, in rice, the localization and function of the OsSEC3a subunit in crown roots depend on lipid-driven PM recruitment of OsEXO70A1 (Zhu et al., 2026). Crucially, the evolutionary timing, functional consequences, and mechanistic underpinnings of the shift in landmarking roles between SEC3 and EXO70 in plants remains unknown.

Over the past decade, considerable effort has been put into understanding the evolution of exocyst complex proteins in land plants, particularly the highly diversified EXO70 subunit (Rawat *et al.,* 2017; Boehm and Field*,* 2019; Žárský *et al.*, 2020). With the increasing availability of recent genomic and transcriptomic data from various streptophyte lineages (Wang *et al.,* 2019; Nishiyama *et al*., 2018; Cheng *et al.,* 2019; Li *et al.,* 2020; Wickell *et al*., 2021), we sought to reassess the plant exocyst evolution and diversification with improved resolution.

Here, we combined phylogenetic reconstruction, cross-species complementation assays, and structural bioinformatics approaches to examine the evolution and diversification of the exocyst complex across streptophytes. By focusing on EXO70, SEC3, and SEC15 homologs from streptophyte alga (*Klebsormidium nitens*), bryophyte (*Marchantia polymorpha*), and tracheophyte model (*Arabidopsis thaliana*), we analyzed the conservation and divergence patterns within the exocyst and experimentally tested functional relationships underlying plasma membrane targeting. Our results indicate that during plant terrestrialization, EXO70.1 subunits became the dominant determinant of exocyst plasma membrane localization at the expense of SEC3.

RESULTS

Exocyst module II shows disproportionate expansion during streptophyte evolution

We collected the exocyst complex subunits homologs from all currently sequenced streptophyte algae and selected land plants (Embryophyta) and reconstructed phylogenetic trees. Among the numerous gene duplications observed across exocyst subunits, only a subset became evolutionarily fixed, therefore generating the new subfamilies (Cvrčková *et al.,* 2012); it is not uncommon for duplications to fail to establish and subsequently vanish. Examination of the two modules that constitute plant exocyst complex (Synek *et. al.,* 2021) revealed that the genes coding for the subunits of the module II expanded extensively during plant evolution-specifically, three of four subunits (SEC15, EXO70 and EXO84) exhibit paralog diversification at distinct stages of streptophyte evolution (Supplementary Fig. S1). While EXO84 subunit diversified to two isoforms in the common ancestor of tracheophytes, SEC15 evolutionarily duplicated in the common ancestor of seed plants/spermatophytes (Supplementary Fig. S1). Notably the EXO70 – the most expanded exocyst subunit – has undergone repeated multiplication and fixation events beginning surprisingly already in the anydrophytes (the common ancestor of zygnematophytes and embryophytes). Crucially, these expansion events continue

in all major plant crown groups (Fig. 1A) – beyond flowering plants, significant EXO70 expansion has occurred also in mosses (crown group of Bryophyta), but even Desmids (crown group of *Zygnematophyceae* algae).

EXO70 triplication in anydrophyta predates land plants and expands independently in several lineages

The EXO70 is the most extensively diversified exocyst complex subunit in land plants. Until recently, genomic analyses were limited largely to flowering plants; consequently, phylogenetic reconstructions of EXO70 evolution captured the paralog expansion characteristic of angiosperms and the basic features of EXO70 subfamilies but missed substantial portions of the paralog proliferation that occurred in other major land plant groups and streptophyte algae (Eliáš *et al.,* 2003; Synek *et al.,* 2006; Chong *et al.,* 2009; Cvrčková *et al.,* 2012; Rawat *et al.,* 2017; Žárský *et al*., 2020).

With the increasing availability of genomes and transcriptomes from these previously undersampled groups (Supplementary Table S1.), we were able to reexamine the EXO70 diversification events in more detail. Strikingly, we found that EXO70 homologs from conjugating algae (Zygnematophyceae) cluster within the three well-defined EXO70 subfamilies originally described in embryophytes (Fig. 1A). This finding extends the origin of three EXO70 subfamilies by tens of millions of years (Su *et al*., 2021) to the anydrophyte lineage (Rensing, 2020). Accordingly, the number of EXO70 paralogs in this group can be found from 6 in *Mesotaenium kramstae* (*Zygnematales*; Fig. 1; Supplementary Fig. S1, S2) to possibly 68 in the *Penium margaritaceum* genome (*Desmidiales;* Jiao *et al*., 2020). As these numerous paralogs are found in the transcriptome assemblies, they are actively expressed, suggesting that they may elaborate on cell morphogenesis. Notably, an independent EXO70 duplication occurred also within the *Charophyceae* - two Chara (*Characeae*) EXO70 homologs are shared also with their *Nitella* relative (*Nitelleae*; Supplementary Fig. S1). Additionally, our data strongly put the root of the EXO70 expansion next to the EXO70.1 family, as summarily indicated by the phylogenetic position orthologs from non-plant models, green algae and pre-anydrophyta streptophyte algae (Fig. 1A, Supplementary Fig. S1).

To gain sequence-independent insight into the early EXO70 evolution, we also analyzed the conservation of exon-intron structure of EXO70s encoding genes from selected members of streptophyte algae and land plants. These data corroborate the evolutionary position of EXO70.1 subfamily (including *Zygnematophyceae*) close to other streptophyte algae and also indicate contrasting modes of evolution between the three subfamilies. While EXO70.1 and EXO70.3 clades evolve primarily by gene duplication, the most diversified subfamily—EXO70.2—likely proliferated through reverse transcription followed by genomic integration as most representatives of the EXO70.2 subfamily are intronless genes (Fig. 1B, Supplementary Fig. S2).

Following the initial triplication in anydrophyta, EXO70 copy number remains low in several early-diverging embryophyte lineages. Hornworts, liverworts, and lycophytes typically encode 3–5 EXO70 homologs (one or two per subfamily), whereas extensive expansion in crown mosses is largely associated with whole-genome duplication events (Rawat *et al*., 2017). Major expansion of the EXO70 family begins in Euphyllophytes. The stepwise manner of these events is evident in Fig. 1 and Supplementary Fig. S1, which also reveals the loss of one evolutionary conserved EXO70.3 clade member (that we termed clade J) in Angiosperms.

Notably, the diversification of EXO70 subunits sequences results in many instances in large shifts in electrostatic charge distribution along the rod-like body of EXO70 molecules. This tendency is most prominent among the 70.2 subfamily representatives (Fig.1) where N'-terminal part of the protein

features prominent negative charge, largely deviating also from the non-plant EXO70s (Fig. 1C).

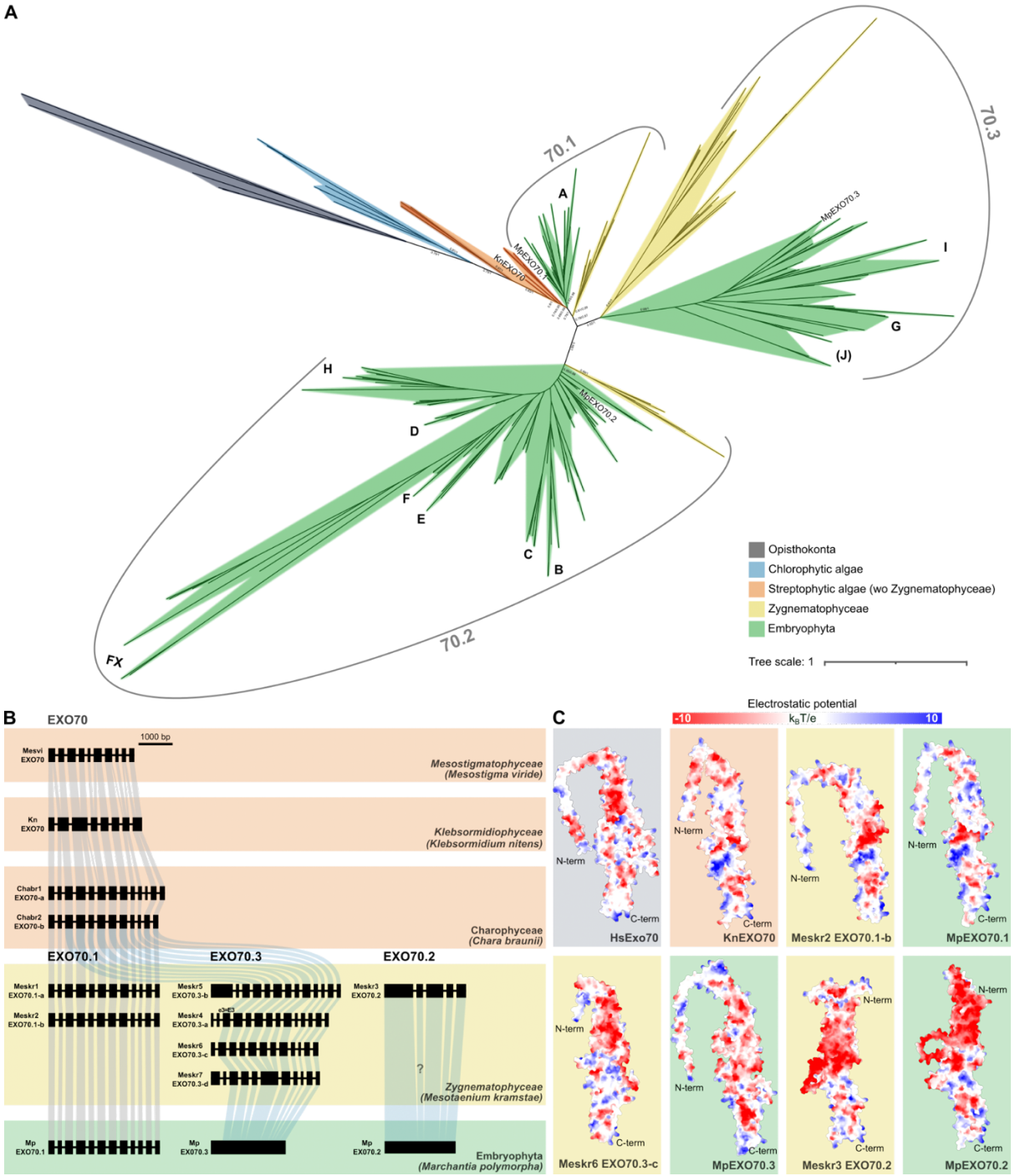

Figure 1. Deep origin and functional diversification of EXO70 subfamilies in streptophytes. A - Phylogenetic analysis of EXO70 proteins across Viridiplantae and representative opisthokont outgroups (see also Supplementary Fig. S1 for more details). **B -** Analysis of gene exon–intron architecture of EXO70 homologs from representative streptophyte lineages. For sake of clarity, intron lengths are not drawn to scale, see Supplementary Fig. S2 for the true scale depiction. **C -** Molecular surface models of selected EXO70 proteins illustrating electrostatic potential distributions across evolutionary lineages and subfamilies. Surface charge is displayed from negative (red) to positive (blue) electrostatic potential. Chabr – *Chara braunii*, Hs - *Homo sapiens*, Kn – *Klebsormidium nitens,* Mp - *Marchantia polymorpha*, Meskr - *Mesotaenium kramstae,* Mesvi – *Mesostigma viride*.

Taken together, our data demonstrate that EXO70 diversification began early in streptophyte evolution, with the establishment of three major subfamilies predating land plant emergence and followed by lineage-specific expansions, distinct duplication mechanisms, and pronounced sequence and structural divergence.

Marchantia encodes three EXO70 genes with distinct localization and overexpression phenotypes

The liverwort *Marchantia polymorpha* possesses only three EXO70 homologs, one representing each of the three EXO70 subfamilies. We took advantage of this minimal EXO70 complement, together with the emerging status of *Marchantia* as a model plant (Bowman et al., 2022), to investigate the evolutionary conservation of EXO70 localization and function using GFP fusion proteins and overexpression approaches. All three *Marchantia* EXO70 genes were N-terminally fused to GFP and expressed under the control of the strong endogenous MpEF1α promoter (Althoff *et al.*, 2014).

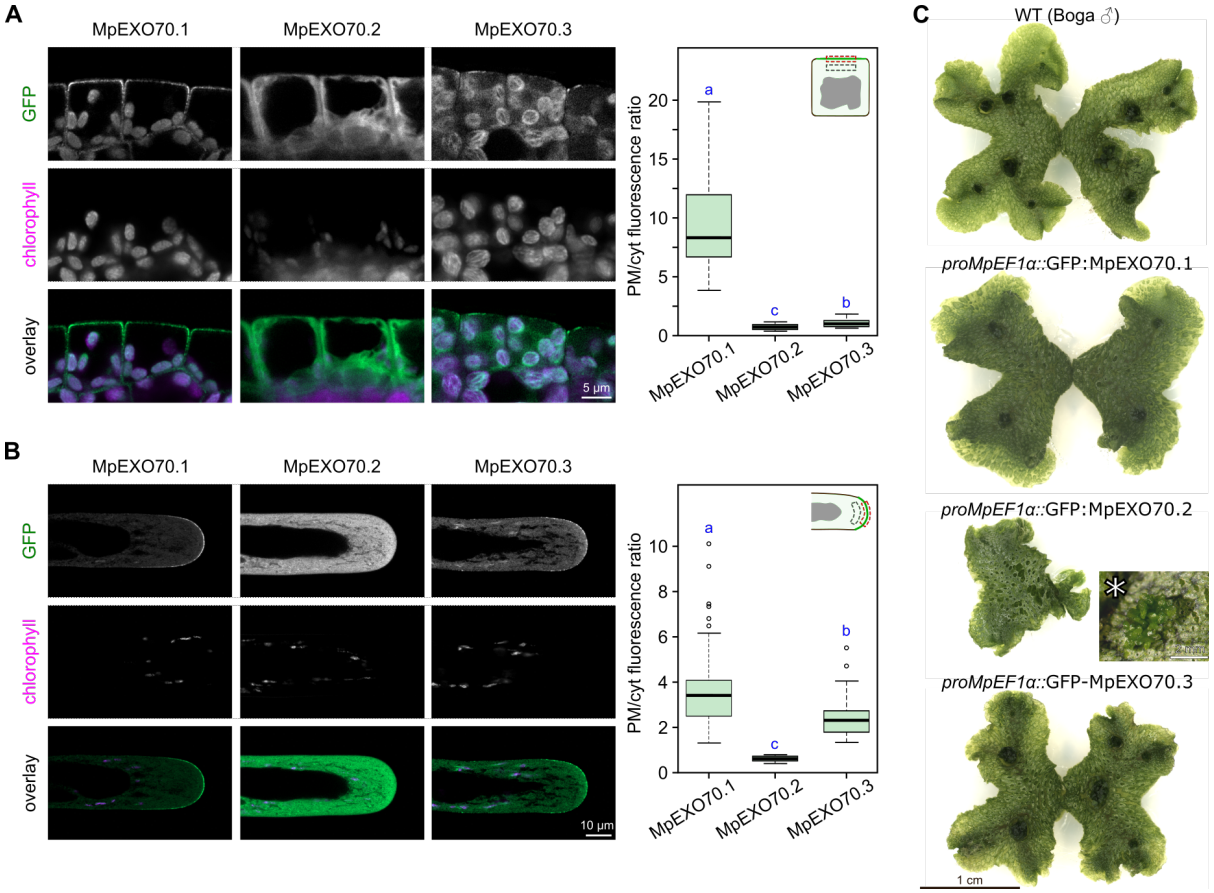

Figure 2. Localization and overexpression analyses of Marchantia EXO70 subfamily representatives in *Marchantia polymorpha*. Localization of GFP-tagged MpEXO isoforms in **A** - gemmae, **B** - rhizoids. GFP, chlorophyll autofluorescence and overlay channels are shown to highlight the true GFP signal. Panels on the right represent the analysis of the PM to cytoplasm (PM/Cyt) fluorescence ratio at the indicated regions. Distinct letters denote statistically different groups (Kruskal-Wallis test with Holm correction, $p < 0.05$). For each line, at least 50 cells from ca. 20 independent gemmae from two independent lines were quantified. **C** - 3 weeks old *in vitro* thallus morphology carrying over-expression constructs (**C*** - gemmae emergence in EXO70.2 over-expressor is delayed and without a gemmae cup, detail with asterisk made after 8 weeks of cultivation). See also Supplementary Fig. S3 for additional details.

The evolutionarily conserved MpEXO70.1 isoform (homologous to AtEXO70A; Fig. 1) localized exclusively to the plasma membrane in thalli, rhizoid initials and rhizoids. In contrast, MpEXO70.2 exhibited predominantly cytoplasmic localization, while MpEXO70.3 displayed a dual plasma membrane–cytoplasmic localization pattern (Fig. 2A, B; Supplementary Fig. S3A, B). Overexpression of MpEXO70.1 and MpEXO70.3 did not produce obvious alterations in overall thallus morphology. By contrast, overexpression of MpEXO70.2 caused severe disruption of thallus architecture, including tearing of the upper epidermis and strongly impaired chloroplast biogenesis. Regenerated thalli of MpEXO70.2 overexpressors were abnormally twisted and lacked gemma cups, with gemmae instead developing directly on the top of the thallus (Fig. 2C; compare also with Supplementary Fig. S3C).

Collectively, our observations highlight pronounced functional and localization differences between the evolutionarily conserved EXO70.1 and the more divergent EXO70.2 and EXO70.3 isoforms in Marchantia polymorpha, that are consistent with their evolutionary relations.

SEC15 subunit shows deep functional conservation within the streptophyte lineage

In contrast to diversification of EXO70 gene family, phylogenetic analysis of the SEC15 subunit across streptophytes revealed that it is typically represented by a single homolog throughout most lineages, until the emergence of seed plants, where it diverged into two stable subfamilies, SEC15A and SEC15B (Supplementary Fig. S1). Notably, SEC15 displays an exceptionally high degree of sequence conservation: across 39 streptophyte sequences, the SEC15 family shows 66% amino acid identity and 79% similarity, with a mean protein length of 808 ± 43 amino acids (Supplementary Dataset S1).

Furthermore, *Arabidopsis* homozygous *sec15b* mutants exhibit pronounced sporophytic phenotypes (Batystová *et al*., 2022).

Given the high level of molecular conservation and clear quantifiable mutant phenotypes, we selected SEC15 as a model subunit to assess functional conservation across streptophytes. For this purpose, we analyzed SEC15 orthologs from *Arabidopsis thaliana*, *Marchantia polymorpha*, and *Klebsormidium nitens*, representing angiosperms, early-diverging land plants, and streptophyte algae, respectively. When expressed under the control of the AtUBQ10 promoter, both the *Marchantia* and *Klebsormidium* SEC15 homologs localized prominently to the lateral plasma membrane domains of rhizodermal cells and to developing cell plates, closely mirroring the localization pattern of AtSEC15B (Fig. 3A). Importantly, both orthologs fully complemented the short etiolated hypocotyl phenotype of the *Arabidopsis sec15b* mutant and restored the overall growth defects associated with loss of AtSEC15B function (Fig. 3B, C).

Together, these results demonstrate that molecular conservation of the SEC15 exocyst subunit correlates strongly with functional conservation across the streptophyte lineage, validating cross-complementation as a robust approach for evolutionary conservation studies.

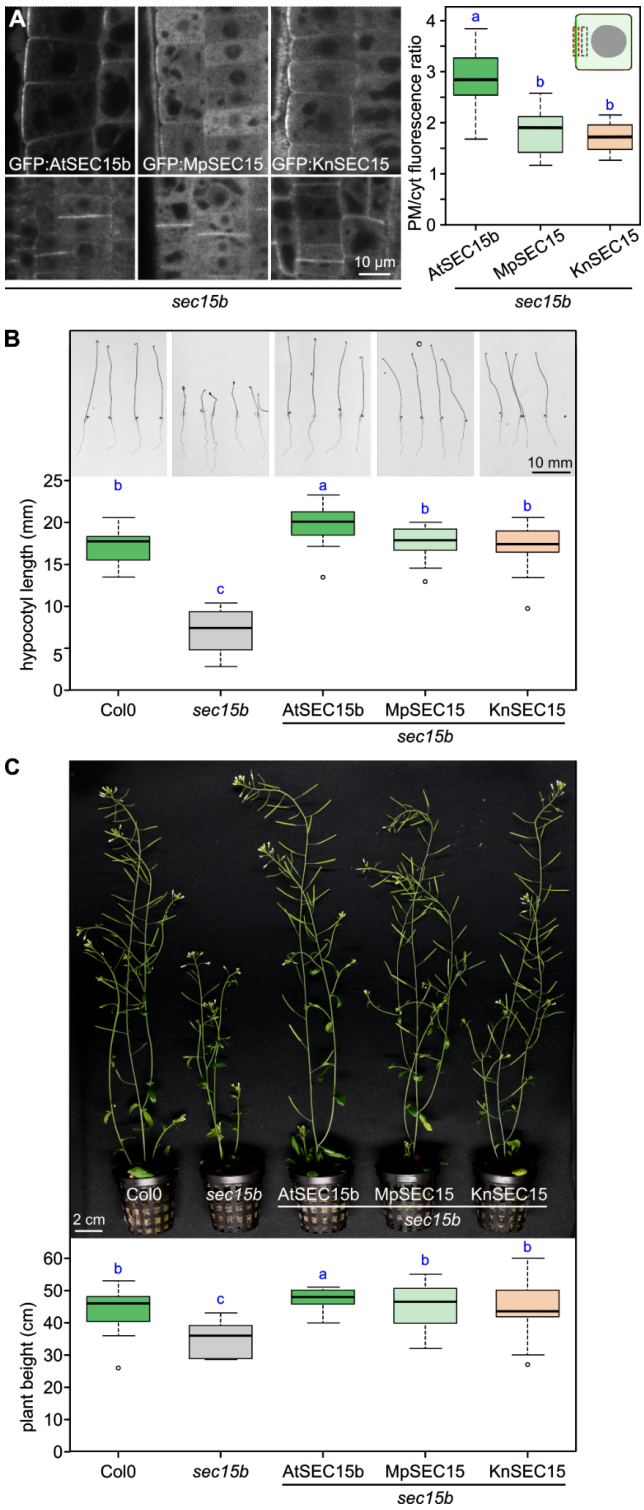

Figure 3. SEC15 orthologs across streptophytes display deep localization and functional conservation. A - Localization of GFP-tagged SEC15 isoforms from Arabidopsis, Marchantia and Klebsormidium in root epidermal cells, focusing on lateral plasma membrane domain and cell plate. The constructs were expressed in the *sec15b* mutant background under the control of Ubq10 promoter. Panel on the right represents the analysis of the PM to cytoplasm (PM/Cyt) fluorescence ratio at the indicated region. For each line, at least 12 cells from four independent plants were quantified. **B** - Representative images and length of 7-day-old etiolated hypocotyls of WT, *sec15b* or *sec15b* seedlings expressing AtSEC15b, MpSEC15 or KnSEC15. For each line, 20 seedlings were quantified. **C** - Representative images and heights of 6-week-old WT, *sec15b* or *sec15b* plants expressing AtSEC15b, MpSEC15 or KnSEC15. For each line, at least 9 plants were quantified. In all plots, distinct letters denote statistically different groups (Kruskal-Wallis test with Holm correction, $p < 0.05$).

EXO70 diversification reveals ancestral conservation and lineage-specific functional specialization in streptophytes

Having established SEC15 as a deeply conserved exocyst subunit whose molecular conservation directly translates into functional interchangeability across streptophytes, we next asked how this paradigm applies to EXO70—the most diversified exocyst component in plants. Since EXO70 underwent early gene multiplication into three distinct subfamilies, the question arises: how does this evolutionary expansion relate to functional conservation and specialization, both within and across EXO70 subfamilies?

To address this, we first examined the subcellular localization and complementation capacity of all three Marchantia polymorpha EXO70 paralogs in Arabidopsis wild-type plants and the *exo70A1* mutant background. All three Marchantia genes were cloned under the constitutive AtUBQ10 promoter, fused to GFP at the N-terminus, and expressed in Arabidopsis. Subcellular localization was subsequently analyzed in root epidermal cells. Consistent with observations in Marchantia, MpEXO70.1 displayed strong enrichment at the lateral plasma membrane domain of rhizodermal cells (Fig. 4A, Supplementary Fig. S4A). Importantly, MpEXO70.1 complemented the severe developmental defects of the Arabidopsis *exo70A1* mutant, restoring overall adult plant architecture and normal developmental progression (Fig. 4B). Moreover, MpEXO70.1 rescued the impaired hypocotyl elongation in dark-grown seedlings and restored normal root hair growth (Fig. 4C, D).

Interestingly, MpEXO70.3 expression resulted in partial complementation across all assessed traits. Although MpEXO70.3-expressing plants remained sterile, exhibited delayed inflorescence initiation, and showed compromised apical dominance similar to the *exo70A1* mutant, they attained greater final height than the mutant, albeit with greater variability than MpEXO70.1-expressing plants (Fig. 4B; Supplementary Fig. S4B). Partial rescue was also observed for hypocotyl elongation in etiolated seedlings and for root hair development (Fig. 4C, D). In sharp contrast, MpEXO70.2, which localized predominantly to the cytoplasm, failed to complement any of the major *exo70A1* mutant phenotypes (Fig. 4B–D).

We next investigated the evolutionary depth of functional conservation within the EXO70.1 clade. Phylogenetic and structural homology analyses indicated that streptophyte algae possessing a single EXO70 homolog—predating the EXO70 gene triplication—cluster close to the EXO70.1 subfamily (Fig. 1A), suggesting that these algal EXO70 proteins may retain the ancestral canonical exocyst subunit function. To test this hypothesis experimentally, we cloned the sole EXO70 homolog from the filamentous streptophyte alga Klebsormidium nitens, representing a sister lineage to Phragmoplastophyta. When expressed in Arabidopsis under the AtUBQ10 promoter, Klebsormidium EXO70 localized both to the cytoplasm and to characteristic exocyst-associated plasma membrane domains at the lateral surface of root epidermal cells, as well as to developing cell plates during cytokinesis (Fig. 4A). Strikingly, Klebsormidium EXO70 complemented all major developmental defects of the Arabidopsis *exo70A1* mutant, including impaired overall growth, hypocotyl elongation, and root hair formation (Fig. 4B–D).

One defining feature controlling EXO70 functionality is its localized electrostatic charge, which is crucial for membrane binding and interactions with other exocyst subunits (Kubátová *et al.*, 2019; Synek *et al.*, 2021; De La Concepcion *et al.*, 2025). We therefore sought to analyze charge distribution across streptophyte EXO70 paralogs and test whether it serves as a distinguishing factor in EXO70 diversification. To this end, we generated AlphaFold models for 59 distinct EXO70 proteins and quantitatively compared their electrostatic surface properties using Protein Interaction Property

Similarity Analysis (PIPSA; Richer *et al.*, 2008), thereby assessing charge distribution similarities and differences across paralogs. PIPSA clustering clearly distinguished members of the three EXO70 subfamilies. Strikingly, single-copy EXO70 paralogs from pre-anydrophyta streptophyte algae (including Klebsormidium) clustered together with land plant EXO70.1 members, consistent with our complementation analysis (Supplementary Fig. S5). Somewhat surprisingly, EXO70.2 and EXO70.3 members from Amborella, Marchantia, and Zygnematophyceae also clustered together with their respective Arabidopsis orthologs, despite their greater evolutionary distance (Supplementary Fig. S5, Supplementary Fig. S1).

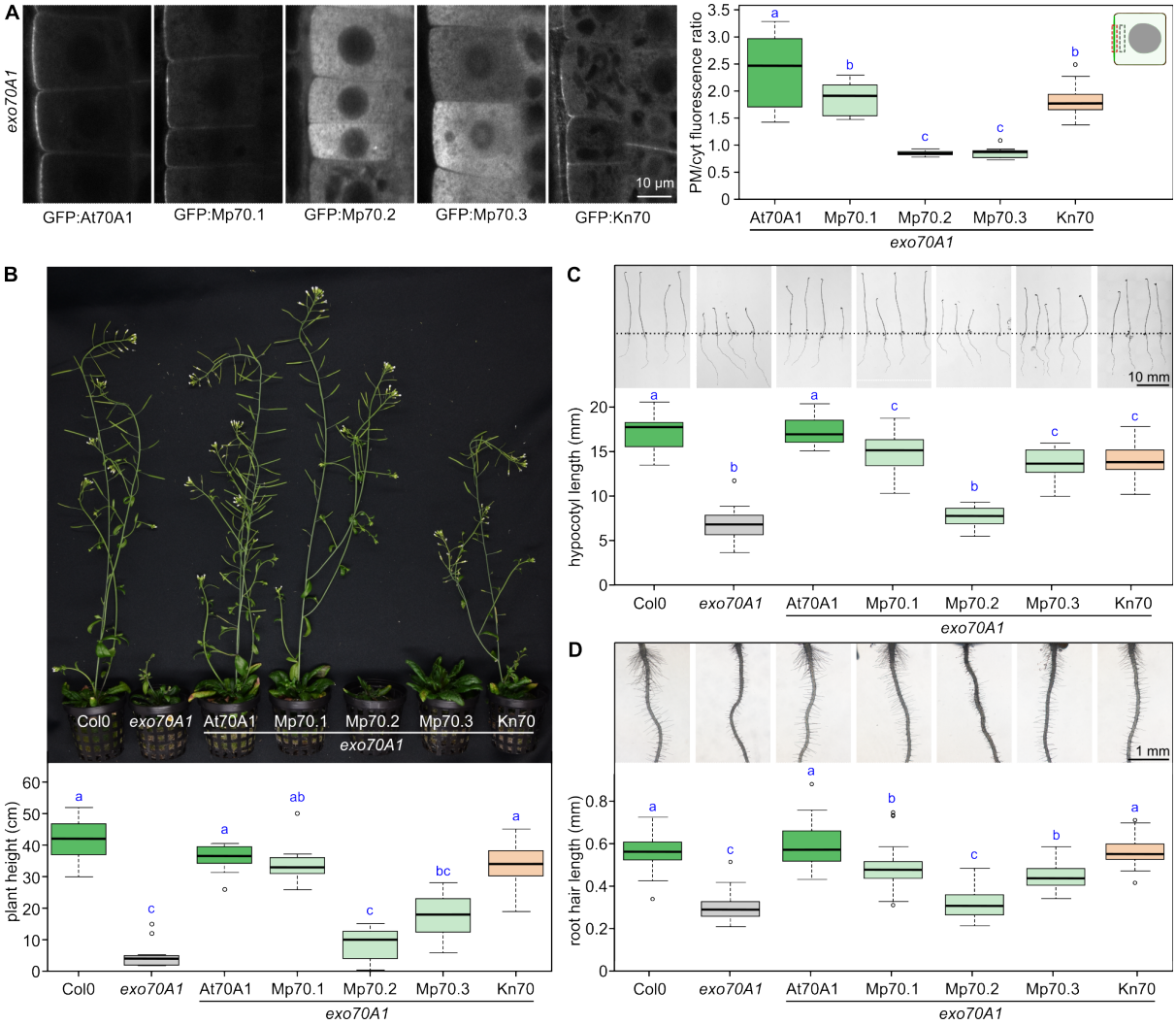

Figure 4. Localization and complementation analyses of Marchantia and Klebsormidium EXO70 homologs in Arabidopsis. A - localization of Arabidopsis EXO70A1, all three EXO70 orthologues from *Marchantia polymorpha* and a single EXO70 ortholog from *Klebsormidium nitens* in Arabidopsis roots of *exo70A1* mutant line. Analysis of the PM to cytoplasm (PM/Cyt) fluorescence ratio at the outer lateral PM in *exo70a1* root epidermal cells. For each line, at least 12 cells from four independent plants were quantified. **B** - Expression of MpEXO70.1 and KnEXO70 largely rescues the dwarf and fertility phenotype of *exo70A1* mutant. For each line, at least 9 plants were quantified. **C** - Multiple Marchantia EXO70 and KnEXO70 restore the hypocotyl elongation defect of the *exo70A1* mutant. For each line, 20 seedlings were quantified. **D** - Marchantia and Klebsormidium EXO70 orthologs display distinct rescue effects on the short root hair growth defect characteristic for the *exo70A1* mutant. For each line, the 5 longest roothairs from 10 seedlings were quantified. In all plots, distinct letters denote statistically different groups (Kruskal-Wallis test with Holm correction, $p < 0.05$). See Supplementary Fig. 4 for additional details.

We therefore next tested whether functional conservation of Marchantia EXO70 paralogs extends beyond the EXO70.1 subfamily and whether the single Klebsormidium EXO70 can function in multiple subfamily contexts. To this end, we assessed their capacity to complement phenotypes of two well-characterized Arabidopsis mutants from the EXO70.2 subfamily: *exo70H4*, which fails to deposit secondary cell wall thickenings in trichomes (Kulich *et al*., 2018), and *exo70B1*, which manifests through early senescence and an anthocyanin accumulation defect (Kulich *et al*., 2013). However, none of the tested Marchantia or Klebsormidium EXO70 paralogs could complement the *exo70H4* or *exo70B1* mutant phenotypes (Supplementary Fig. S4C–E), indicating lineage-specific functional diversification within the EXO70.2 subfamily.

Together, these results demonstrate that EXO70 diversification in land plants led to pronounced functional divergence among paralogs. The canonical EXO70 function—possibly underpinned by conserved surface charge distribution—was retained by the EXO70.1 lineage and is already present in streptophyte algae, predating plant terrestrialization. Conversely, the specialized functions of Arabidopsis EXO70.2 subfamily members could not be complemented by either MpEXO70.2 or KnEXO70, indicating that these functions evolved independently in distinct land plant lineages.

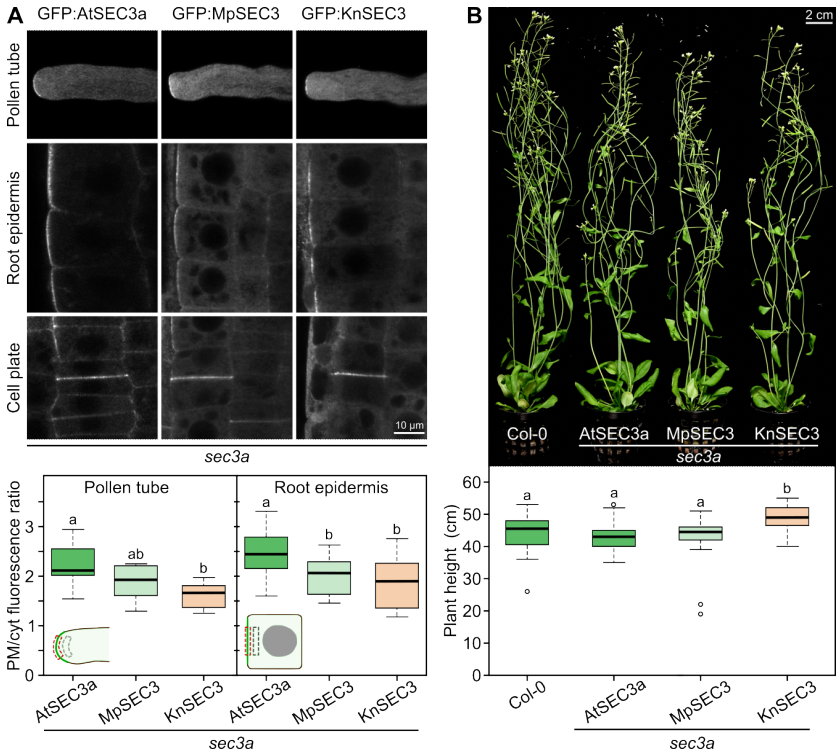

Figure 5. Localization and complementation analyses of native, Marchantia and Klebsormidium SEC3 homologs in Arabidopsis *sec3a* mutant. A - Localization of GFP-tagged SEC3 isoforms from Arabidopsis, Marchantia and Klebsormidium in growing pollen tubes, lateral plasma membrane domain of root epidermal cells, and cell plates. The constructs were expressed in the *sec3a* mutant background under the control of Ubq10 promoter. Panel below the micrographs represents the analysis of the PM to cytoplasm (PM/Cyt) fluorescence ratio in pollen tubes and root epidermis at indicated regions. For each line, at least 6 pollen tubes were quantified and 12 root epidermal cells from four independent plants were quantified. **B** - Representative images and heights of 6-week-old WT, and *sec3a* plants expressing AtSEC3a, MpSEC3 or KnSEC3. For each line, at least 15 plants were quantified. In all plots, distinct letters denote statistically different groups (Kruskal-Wallis test with Holm correction, $p < 0.05$). See Supplementary Fig. S6 for more details.

SEC3 retains ancestral membrane targeting capacity in streptophytes but becomes EXO70-dependent in embryophytes

Studies in fungal and animal systems have established the exocyst subunit SEC3, together with EXO70, as a key determinant of exocyst targeting to specific plasma membrane domains. In these systems, membrane targeting relies on coordinated interactions with membrane lipids and small GTPases, providing a critical "landmarking" function for exocyst assembly and activity (Boyd *et al*., 2004; Wu *et al.*, 2008; Pleskot *et al*., 2015). In contrast, although SEC3 remains essential for exocyst function in plants, its landmarking role appears diminished in *Arabidopsis* (Bloch *et al*., 2016). Building on our analyses of SEC15 and EXO70, we therefore sought to comparatively assess the functional contribution of SEC3 to exocyst localization and activity across the streptophyte lineage. To this end, we transformed heterozygous *Arabidopsis sec3a* mutants with GFP-tagged SEC3 homologs from *Arabidopsis thaliana*, *Marchantia polymorpha*, and *Klebsormidium nitens*, expressed under the constitutive AtUBQ10 promoter.

SEC3 homologs from all three species exhibited highly similar localization patterns, accumulating at the lateral plasma membrane domains of root epidermal cells, at maturing cell plates, and at the tips of growing pollen tubes (Fig. 5A). Consistent with this conserved subcellular localization, both *Marchantia* and *Klebsormidium* SEC3 homologs fully complemented the *Arabidopsis sec3a* pollen transmission defect and restored wild-type growth (Fig. 5B; Supplementary Fig. S6), demonstrating deep functional conservation of SEC3 across streptophytes.

To directly compare the relative contributions of SEC3 and EXO70 to exocyst membrane targeting during evolution, we next examined the behavior of SEC3 homologs in the *Arabidopsis exo70A1* mutant background, extending previous observations indicating an increased reliance on EXO70.1 for plasma membrane targeting in land plants (Bloch et al., 2016; Synek *et al*., 2021). Strikingly, whereas the *Arabidopsis* and *Marchantia* SEC3 proteins were displaced from the plasma membrane and accumulated in cytoplasmic patches in the *exo70A1* mutant (identical to those previously described in Synek *et al*., 2021), *Klebsormidium* SEC3 retained partial plasma membrane localization in the absence of EXO70A1 (Fig. 6A, B). We confirmed that this residual membrane association occurred within the context of the assembled exocyst complex, as evidenced by co-immunoprecipitation of endogenous SEC6 with *Klebsormidium* SEC3 (Fig. 6C).

Consistent with these localization differences, independent *Klebsormidium* SEC3 lines partially but robustly complemented the severe growth and developmental defects of the *Arabidopsis exo70A1* mutant, including restoration of fertility and seed production. In contrast, neither *Arabidopsis* nor *Marchantia* SEC3 homologs provided detectable complementation in the *exo70A1* background (Fig. 6D–F).

Taken together, these results indicate that while SEC3 remains functionally conserved across streptophytes, its contribution to exocyst plasma membrane targeting has been progressively reduced during land plant evolution. We propose that, concomitant with the multiplication and diversification of EXO70 paralogs, EXO70.1 became the dominant determinant of exocyst membrane targeting in embryophytes, whereas SEC3 retained this capability only in early-diverging streptophyte lineages.

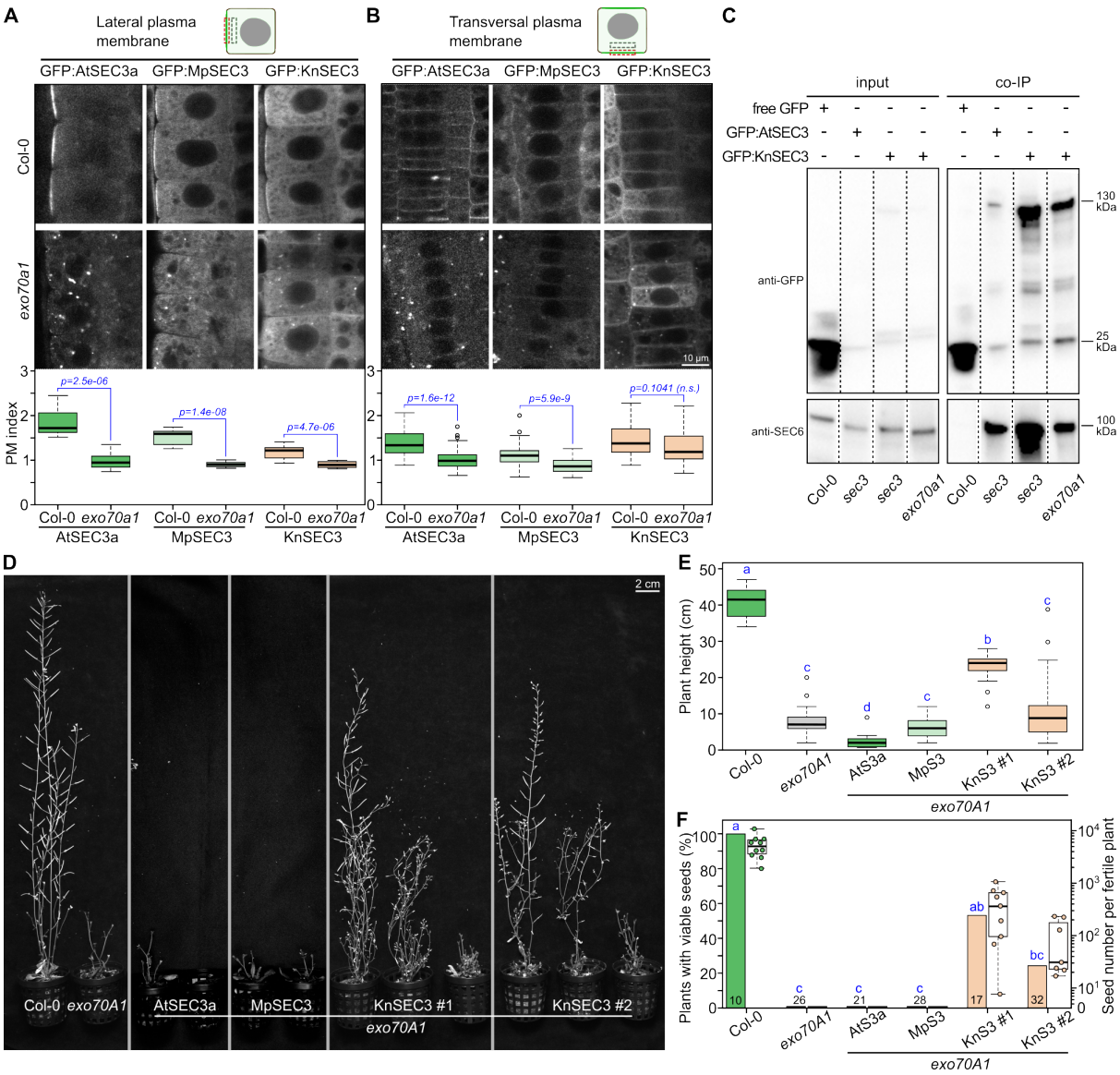

Figure 6. Evolutionary shift in SEC3-mediated exocyst membrane targeting. A, B - Localization of GFP-tagged SEC3 isoforms from Arabidopsis, Marchantia and Klebsormidium in wild-type and *exo70A1* mutant background. Analysis of the PM to cytoplasm (PM/Cyt) fluorescence ratio at the outer lateral PM in the root epidermal cells (**A**) or at the transversal PM in cortical cells (**B**). Klebsormidium SEC3 still partially localizes to the plasma membrane in Arabidopsis *exo70A1*. Statistical significances from Mann-Whitney U tests are indicated. **C** - Co-immunoprecipitation of the exocyst core subunit SEC6 with GFP-tagged AtSEC3a and KnSEC3 in wild-type, *sec3a*, and *exo70A1* mutant backgrounds. Detection of SEC6 in SEC3 immunoprecipitates confirms association of both Arabidopsis and Klebsormidium SEC3 with the exocyst complex, including in the *exo70a1* background. Input and co-IP controls are shown. **D, E** - Klebsormidium SEC3 partially complements *exo70A1* mutant growth defects. Representative plant images (**D**) and quantitative analysis of plant height (**E**) show significant, though incomplete, rescue by two independent KnSEC3 lines compared to exo70a1 mutants and Arabidopsis or Marchantia SEC3 expression.For each line, at least 10 plants were quantified. **F** - Expression of Klebsormidium SEC3 increases the fertility of *exo70A1*. The number of plants analyzed is indicated at the bottom of the graph. Distinct letters above boxplots denote statistically different groups (Kruskal-Wallis test with Holm correction, $p < 0.05$). See Supplementary Fig. S6 for additional details.

Structural Plasticity of the Exocyst Enables EXO70-Independent Function via Klebsormidium SEC3

To gain molecular insight into why Klebsormidium SEC3 performs better than land-plant SEC3 orthologs in the Arabidopsis background lacking EXO70, we analyzed its sequence and structural features. Multiple-sequence alignment of SEC3 did not reveal distinctive motifs that set Klebsormidium SEC3 apart from land-plant orthologs. Likewise, structural surface analysis of the N-terminal PH domain—critical for membrane binding in yeast (Pleskot *et al*., 2015) but dispensable in Arabidopsis (Bloch *et al*., 2016)—did not indicate altered membrane-binding capability for the Klebsormidium ortholog (data not shown). These observations suggested that the positive effect of Klebsormidium SEC3 manifests in the context of the assembled exocyst complex. To explore this possibility, we employed the AlphaFold3 (AF3) algorithm (Abramson *et al*., 2023), followed by comparative structural analyses of predicted exocyst complexes.

Using the methodology trained on the Saccharomyces cerevisiae exocyst structure (Supplementary Fig. S7), we then predicted near full-length structures of exocyst complexes from Arabidopsis, Marchantia, and Klebsormidium (covering 85–95% of residues), as well as Arabidopsis variants lacking EXO70A1 and harboring SEC3 from Arabidopsis, Marchantia, or Klebsormidium (Supplementary Figs. S7, S8A-D). Independent predictions converged on a globally similar architecture comprising two modules, which are strongly coupled by interfaces among the positionally well-supported subunits SEC5, SEC8, SEC15, and EXO84 (Fig. 7A–D; Supplementary Fig. S7). Notably, SEC3 and EXO70 (and, to a lesser extent, SEC6 and SEC10) are tightly integrated via their N-terminal CorEX motifs, yet their overall positions within the complex are poorly supported, indicating structural flexibility. Predictions for Arabidopsis and Marchantia complexes containing EXO70 subfamily 70.2 and 70.3 members suggested even greater positional variability, particularly for EXO70.2 proteins (Arabidopsis EXO70B1, EXO70H4, and Marchantia EXO70.2).

Comparative modeling of Arabidopsis exocyst assemblies lacking EXO70A1 and containing SEC3 from different species yielded structures globally similar to the native Arabidopsis complex but with higher ipSAE subunit–subunit scores, indicative of a more compact organization and reduced separation between the two modules (Supplementary Fig. S8A-D). When we contrasted quantitative features of functional complexes—the native Arabidopsis exocyst and the EXO70A1-deficient complex carrying Klebsormidium SEC3—with non-functional EXO70A1-deficient assemblies containing either Arabidopsis SEC3 or Marchantia SEC3, we observed that the non-functional complexes formed novel SEC5–SEC10 and SEC5–EXO84 interfaces absent from the functional variants (Fig. 7E). Detailed inspection showed that these aberrant interfaces are confined to the N-terminal CorEX motifs (Fig. 7F), where increased numbers of SEC5–SEC10 and SEC5–EXO84 contacts generate pronounced interactions between module I and module II. On the other hand, these interfaces are substantially looser in the functional exocyst variants (Fig. 7H). Importantly, a similarly low contact number—and a loosened inter-module interface—is also observed in the model of the native *Klebsormidium* exocyst complex (Fig. 7G; Supplementary Fig. S8E). Although we could not identify individual sequence features of *Klebsormidium* SEC3 that directly account for these structural differences, we noted that the N-terminal region of *Klebsormidium* SEC3 proximal to the affected SEC5 region (KnSEC3 residues 219–319) is enriched in small, non-charged amino acids relative to corresponding regions of land-plant SEC3 orthologs.

Together, our comparative analysis indicates that Klebsormidium SEC3 promotes a more permissive and dynamic interface between module I and module II of the exocyst complex. By preventing the formation of aberrant, overly stabilizing contacts between SEC5, SEC10, and EXO84, Klebsormidium

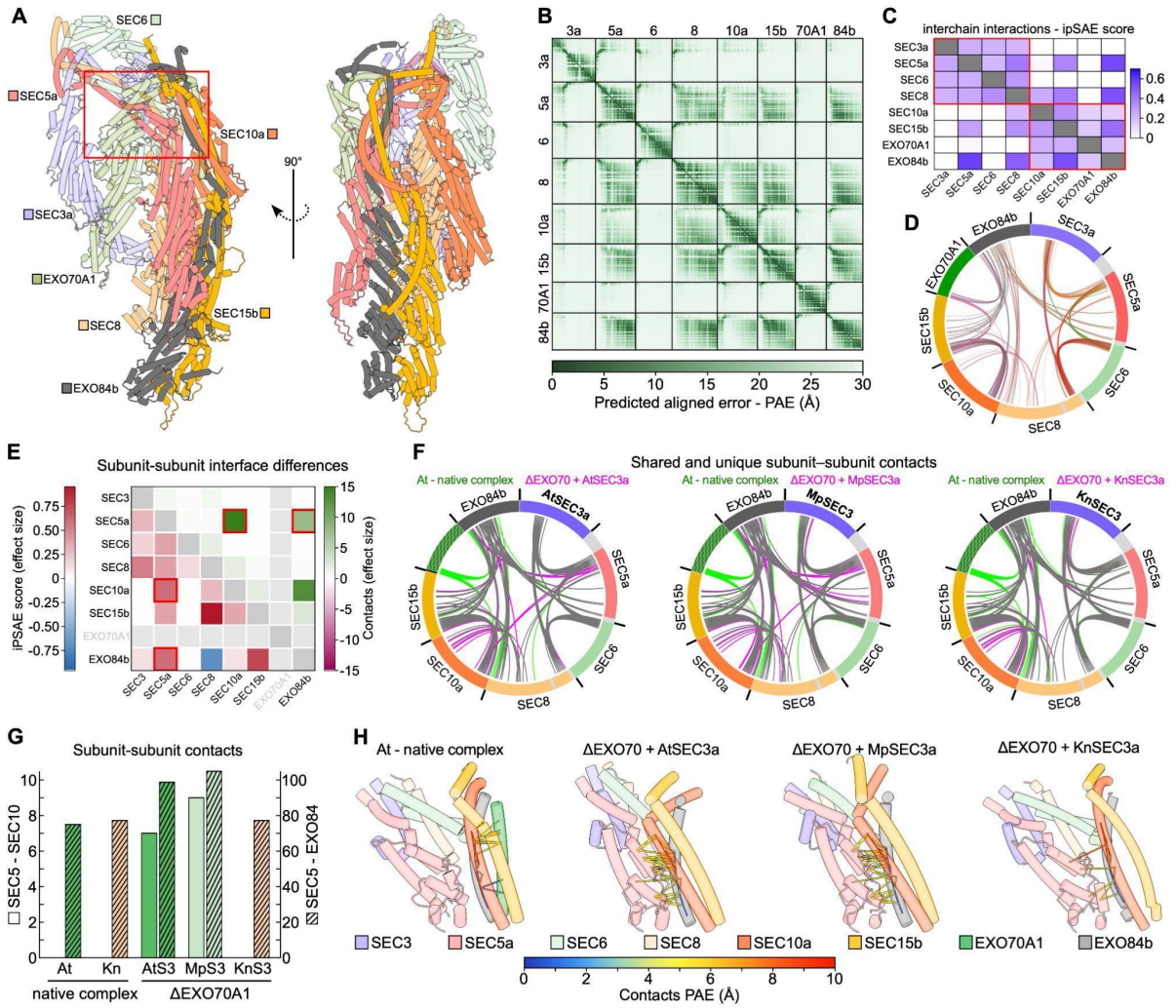

Figure 7. Comparative Structural Analysis of Exocyst Complexes Reveals a Unique Role for Klebsormidium SEC3. A - schematic representations of the Alphafold3 (AF3) exocyst model from *Arabidopsis thaliana*. Subunits with uncertain global position are shown as semi-transparent. Red rectangle indicates the position of CorEX helical bundles. **B** - Predicted aligned error (PAE) plots for Arabidopsis exocyst from AF3 prediction showing model confidence in relative residue positioning, with low (dark green) and high (light green) PAE values indicating robustly predicted rigid regions and versus flexible or uncertain regions, respectively. **C** - Heatmap showing the ipSAE (interaction prediction Score from Aligned Errors) for the individual subunit-subunit interfaces computed for the Arabidopsis exocyst with the 10 Å threshold. Red rectangles indicate the interactions within module I and II, respectively. **D** - chord plot projection of inter-subunit contacts for Arabidopsis exocyst complex. Inter-subunit residue-residue contacts with distance < 5 Å and predicted aligner error (PAE) < 10 Å are indicated. Regions trimmed before modelling are shown in grey. **E** - Heatmap showing differences in ipSAE metrics and inter-subunit contacts between functional and non-functional exocyst variants, presents as Cohen's d effect sizes. Red rectangles indicate SEC5-SEC10 and SEC5-EXO84 interactions. **F** - Differential inter-subunit contacts between models for native Arabidopsis complex and variants lacking EXO70A1 and harboring SEC3 from Arabidopsis, Marchantia, or Klebsormidium. Shared contacts are in grey, contacts specific for the native complex in green and contacts specific for the ΔEXO70A1 variants are in magenta. **G** - Number of interface contacts between SEC5-SEC10 and SEC5-EXO84 subunits. **H** - Close-up visualization of robustly predicted contacts between subunits of modules I and II. The visualised region corresponds to the boxed rectangle from panel A. Only contacts with distance < 5 Å and PAE < 10 Å are shown.

SEC3 maintains a looser inter-module architecture, thus preserving exocyst functionality even in the absence of EXO70.

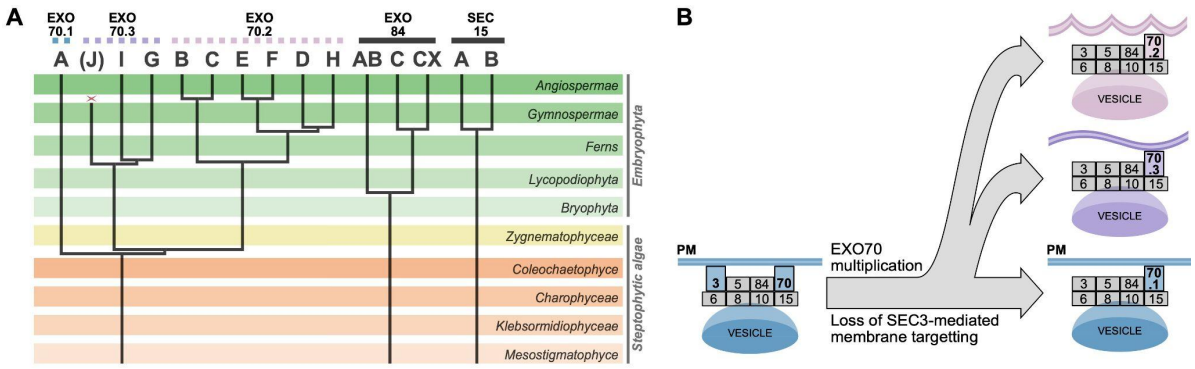

Figure 8. Early EXO70 diversification shapes plant exocyst function. A - Schematic summary of cladistic phylogenetic analyses illustrating the emergence and diversification of selected module II exocyst subunits (EXO70, EXO84, and SEC15) during streptophyte evolution. **B** - Hypothetical model depicting a plant-specific evolutionary shift of exocyst membrane-targeting mechanisms. In evolutionary distant streptophyte algae, SEC3 contributes directly to plasma membrane (PM) association of the exocyst complex, together with EXO70. During embryophyte evolution, this contribution is reduced, coincident with EXO70 multiplication and functional specialization. In land plants, EXO70.1 emerges as the dominant determinant of exocyst membrane localization to plasma membrane, while SEC3 becomes increasingly dependent on EXO70 for effective PM targeting. This redistribution is proposed to have enabled paralog-specific recruitment of the exocyst complex or exocyst-derived subassemblies to distinct membrane domains.

DISCUSSION

Exocyst evolution in streptophytes reveals asymmetric constraint within a conserved complex

The exocyst is a conserved tethering complex whose core subunit composition predates the divergence of major eukaryotic lineages (Boehm and Field, 2019), while retaining fundamental roles in exocytosis and possibly also in autophagy (Žárský, 2022; Kumari et al., 2025). Our streptophyte-wide analysis reveals, however, that individual exocyst subunits have experienced markedly different evolutionary constraints. These differences converge at the level of the two exocyst modules and define two principal evolutionary axes discussed below: diversification of EXO70 within module II, and a plant-specific redistribution of membrane-targeting roles between SEC3 and EXO70.

Across all streptophyte lineages, the copy number of module I subunits mostly remains constrained to one or two per subunit, whereas most module II subunits diversified extensively during plant evolution (Fig. 8A). The earliest and most pronounced expansion involves EXO70, beginning in anydrophytes, followed by duplication of EXO84 at the base of tracheophytes and subsequent diversification in crown lineages (Fig. 8A; Supplementary Fig. S1). A further module II innovation is the duplication of SEC15 in spermatophytes. While the functional significance of EXO84 duplication remains unclear, we hypothesize that SEC15 duplication in seed plants may be linked to increasing functional differentiation between sporophytic and gametophytic programs and to processes associated with sexual reproduction (Batystová et al., 2022). Together, this asymmetry indicates that plant exocyst evolution proceeded not by uniform modification of the entire complex, but by the generation of multiple module II variants that interact with a comparatively constrained module I to support distinct cellular functions.

Early EXO70 multiplication predates land plants and retains a canonical EXO70.1 lineage

Previous phylogenetic studies placed the emergence of the three major EXO70 subfamilies in the common ancestor of embryophytes (Synek et al., 2006; Cvrčková et al., 2012; Žárský et al., 2020). Our analyses extend this origin deeper, to anydrophytes—the common ancestor of embryophytes and zygnematophytes (Rensing, 2020). This timing places EXO70 diversification at a critical evolutionary transition preceding or at the dawn of land colonization. In anydrophytes, duplication of an ancestral single EXO70 was rapidly followed by a second duplication, yielding the three clades—EXO70.1, EXO70.2, and EXO70.3—whose topology is conserved in both zygnematophytes and embryophytes (Fig. 1; Fig. 8A).

To test functional consequences of this diversification, we exploited cross-species complementation using SEC3, SEC15, and EXO70—subunits representing contrasting evolutionary trajectories from both modules—and three phylogenetically distant species: *Klebsormidium nitens* (streptophyte alga), *Marchantia polymorpha* (bryophyte), and *Arabidopsis tahliana* (tracheophyte). Single homologs of SEC3 and SEC15 from Klebsormidium and Marchantia localized to the plasma membrane in Arabidopsis and fully complemented *sec3a* and *sec15b* mutants, confirming deep functional conservation of these subunits. In contrast, EXO70 paralogs showed striking functional divergence. Klebsormidium EXO70 and Marchantia EXO70.1 fully complemented the *exo70a1* mutant, whereas MpEXO70.3 showed partial localization and rescue, and cytoplasmic MpEXO70.2 failed to complement.

These results demonstrate that canonical EXO70 function was already established in streptophyte algae and retained in the EXO70.1 lineage. Notably, although algal EXO70 proteins fall outside the EXO70.1 clade phylogenetically, they cluster with EXO70.1 in protein surface charge analyses, underscoring the importance of conserved electrostatics for membrane association and protein–protein interactions (Zhou and Pang, 2018). Together with correlating localization patterns and contrasting overexpression phenotypes of the three paralogs in Marchantia, these findings reveal deep functional divergence among the basal EXO70 subfamilies.

EXO70 diversification and exocyst association

Recently, De La Concepción et al. (2025) proposed that EXO70 diversification was enabled by electrostatic shifts in the CorEX N-terminal region that reduce its stable association with the exocyst ("complex escape"), with evolutionarily later reassociation invoked to explain exocyst binding by some Arabidopsis EXO70.2 members. In Marchantia, this model is supported by the predominantly cytosolic localization of EXO70.2 during cytokinesis, contrasted with EXO70.1 and EXO70.3 enrichment at the cell plate alongside core subunits.

Our data are consistent with several core observations of this framework, including the functional and localization separation of the three *Marchantia* paralogs and the superior ability of MpEXO70.1 (and partially MpEXO70.3) to substitute for canonical EXO70A1-dependent functions in Arabidopsis. At the same time, evidence from angiosperms indicates that the relationship between EXO70 diversification and exocyst association is more heterogeneous than a simple dichotomy between complex-bound and complex-free states. Several EXO70.2 paralogs implicated in defense, autophagy, and specialized secretion (EXO70B1, EXO70B2, EXO70E2) show physical or functional association with core subunits, whereas others (EXO70C1/C2) appear largely excluded from the complex and may antagonize secretion (Pečenková et al., 2011; Kulich et al., 2013; Synek et al., 2017; Brillada et al., 2022; Michalopoulou et al., 2022; Ortmannová et al., 2022). This pattern points to fine-grained specialization in the degree and context of exocyst engagement within the EXO70.2 subfamily.

Importantly, exocyst-independent EXO70 functions do not necessarily require permanent dissociation from the complex. In opisthokonts, EXO70 exists in both free and exocyst-incorporated pools, with the free pool contributing to membrane deformation and curvature generation (Zhao et al., 2013; Morgera et al., 2012). EXO70 paralogs may diversify primarily by modulating their equilibrium between free and complex-associated states, rather than by complete evolutionary disengagement.

Plant exocyst function also extends beyond canonical secretion associated with primary cell wall formation. Functional specificity among EXO70.2 paralogs is particularly striking, as closely related isoforms are frequently non-interchangeable in vivo, indicating specialization for distinct trafficking pathways and membrane domains (Sekereš et al., 2015; Kulich et al., 2018; Marković et al., 2021). We hypothesize that this specialization reflects differential recruitment of exocyst assemblies to pathway-specific membrane environments rather than uniform "escape" from the complex.

Collectively, these findings support a model in which early EXO70 triplication provided a platform for functional diversification of exocyst activity. Differential electrostatic properties of EXO70 paralogs likely modulate the stability, geometry, and context of exocyst association, enabling lineage- and pathway-specific solutions. Within this view, the complex escape model and our data represent complementary perspectives on how electrostatic tuning and regulatory plasticity shaped EXO70 evolution in plants.

Plant-specific redistribution of exocyst membrane targeting: from SEC3 contribution to EXO70.1 dominance

In parallel with EXO70 multiplication, we identify a second major evolutionary transition: a weakening of SEC3's autonomous contribution to plasma membrane targeting in favor of EXO70.1 dominance. This redistribution emerges as a defining feature of embryophyte exocyst organization.

Early evidence for this shift came from studies showing that the N-terminal PH domain of Arabidopsis SEC3a, previously assumed to mediate membrane binding, is dispensable for SEC3 function. An N-terminally truncated SEC3 lacking membrane-binding capacity fully complemented *sec3a* pollen tube defects (Bloch et al., 2016). Consistently, plasma membrane localization of SEC3a—and of the exocyst complex as a whole—is strictly dependent on EXO70.1 in Arabidopsis (Synek et al., 2021), a dependency we now extend to Marchantia. A direct interaction between SEC3 and EXO70A1, first reported in Arabidopsis (Hála et al., 2008) and absent from opisthokont systems, further supports a plant-specific strengthening of SEC3–EXO70 coupling. Recent work in rice independently corroborates this conclusion by showing that SEC3a function in crown root formation depends on EXO70A1 association (Zhu et al., 2026).

Strikingly, this dependence does not apply to the evolutionarily distant streptophyte alga Klebsormidium. In an Arabidopsis *exo70a1* background, Klebsormidium SEC3 retains partial plasma membrane localization and partially rescues mutant phenotypes. Comparative AF3-based modeling suggests a mechanistic explanation: while both exocyst modules form stable cores across species, SEC3 and EXO70 occupy flexible global positions. The presence of Klebsormidium SEC3 results in fewer stabilizing inter-module contacts, leading to a looser architecture that may permit partial membrane landmarking in the absence of EXO70A1. Although predictive, these observations suggest that SEC3 sequential or structural features can tune inter-module plasticity and thereby modulate reliance on EXO70.

In summary, we conclude that embryophyte exocyst evolution involved a coordinated process in which EXO70 triplication coincided with a redistribution of membrane-targeting capacity from SEC3 to EXO70.1 (Fig. 8B). This shift likely enabled different EXO70 paralogs to direct the exocyst complex—or exocyst-derived subassemblies—to distinct membrane domains and cellular processes.

MATERIALS AND METHODS

Sequence retrieval and analyses

The goal was to acquire at least two species from each major evolutionary group (namely *Mesostigmatophyceae*, *Klebsormidiophyceae*, *Charophyceae*, *Zygnematophyceae*, *Anthocerotophyta*, *Marchantiophyta*, true *Bryophyta*, *Lycopodiophyta*, *Monilophyta* (Ferns), *Gymnosperms* and *Angiosperms*), to create balanced and largely representative datasets. The sequences have been retrieved from publicly available genome and transcriptome databases (Table S1). Sequences from the genome releases were revisited with transcriptome assemblies within the identical species or genus and occasionally accordingly reassembled using FGENESH+ (Solovyev, 2006). MUSCLE (Edgar, 2004) or Mafft (Katoh and Standley, 2013) algorithms were used for the multiple alignments generation, and maximum likelihood algorithm in PhyML (Guindon *et al.,* 2010) was employed for the phylogenetic tree recontruction with LG+G4 settings, implemented in the SeaView multiplatform program (Gouy *et al.,* 2010).

Constructions of binary vectors

To fit our needs, pMpGWB101 binary vector (Addgene #68555) has been cut by *BamHI* and *SacI* and modified using Annealed Oligo Cloning method (using P1+P2, Table S2.). Subsequently, *proMpEF1α* (P3+P4, Table S2.), *proAtUBQ10* (P5+6, Table S2.) and GFP (P7+P8, Table S2.) have been PCR amplified and ligated into the backbone using *HindIII*, *NcoI* and *BamHI* restriction enzymes. All the exocyst subunits were ligated N-terminally to the GFP using *BamHI/XmaI*-CDS-*PacI* restriction sites (P11-P36, Table S2.).

Plant materials and growth conditions

The *Marchantia polymorpha* BoGa male strain has been maintained on ½-strength Gamborg medium solidified with 1.2% agar (Gamborg et al., 1968; Duchefa Biochemie) in a cultivation room at 22 °C under a 16/8 h light/dark regime with a light intensity of approximately 185 µmol photons m^{-2} s^{-1}. For the transformation, G – AgarTrap method has been used (Tsuboyama and Kodama, 2018) with selection on 10 $\mu g.ml^{-1}$ Hygromycin and 100 $\mu g.ml^{-1}$ Claforan.

Arabidopsis thaliana seeds were surface sterilised, stratified for 2d at 4°C and germinated on vertical ½ Murashige-Skoog supplemented with 1% sucrose, vitamin mixture, and 1.6% plant agar (Duchefa Biochemie) at the same regime as mentioned above. Young seedlings were transferred to pellets (Jiffy Products International) and moved to *ex vitro* (22 °C, 16/8 light/dark regime). In this study Arabidopsis mutants *exo70A1* (SALK_014826; Synek et al., 2006), *exo70H4* (SALK_023593, Kulich *et al.*, 2015), *exo70B1* (GK-156G02, Kulich *et al.*, 2013.) *sec15b* (SALK_130663 , Batystová *et al.*, 2022) and *sec3a* (GABI_652H12; Bloch *et al.*, 2016) were used. Genotyping of mutants was performed using the following primer combinations (Table S2): *exo70A1* P31+P33, P31+P32; *exo70H4* P34+P35, P35+P33; *exo70B1* P36+P37, P37+P40; *sec15b* P38+P39, P39+P33; *sec3a* P31+P32+P36. Transgenic lines of *Arabidopsis thaliana* were generated using *Agrobacterium tumefaciens* GV3101 strain by floral dip

method (Clough and Bent; 1998). To evaluate the complementation capacity of evolutionary distinct variants of exocyst subunits, we analyzed their functionality in the second generation of transformed *exo70a1* or *sec3a* heterozygotes. GFP-positive seedlings were visually selected and transferred to soil. The phenotype was documented 8 weeks after germination. Plant height was measured at the post-flowering stage because *exo70A1* mutant plants exhibit delayed flowering.

Arabidopsis pollen tube germination

Pollen grains were germinated on solid medium containing 10% sucrose, 0.01% H_3BO_3, 5 mM $CaCl_2$, 1 mM $MgSO_4$, 5 mM KCl, and 1.5% low-melting agarose (pH 7.5). Petri dishes with pollen grains were incubated inverted at room temperature for 3–5 h. Agarose blocks with germinated pollen tubes were excised and transferred to a microscopy chamber for observation.

Microscopic observations and quantification

Subcellular localizations of selected fluorescently tagged exocyst subunits were examined in young Arabidopsis roots (7d) and Marchantia gemmae using ZEISS LSM 900 (JENA/Germany) equipped with Airyscan 2 using a 488/561 nm laser (objective: LD LCI Plan-Apo 40x/1,2 Imm Corr DIC M27, Plan-Apochromat 63x/1.40 Oil DIC M27, alpha Plan-Apochromat 100x/1.46 Oil DIC M27).

In vitro thallus of *Marchantia polymorpha* and etiolated seedlings of *Arabidopsis thaliana* were imaged on Stereomicroscope Leica M205FA (objective Plan-Apochromat 2x, camera Leica DMC6200 colour 2.2Mp)

Root hairs were imaged on Olympus BX51 stereo binocular microscope (objective Olympus UplanApo 4x NA 0,16, camera Olympus DP74).

For post-acquisition image processing and for all quantifications Fiji software was used (Schindelin *et al*., 2012). Figures were prepared in Inkscape. The PM association was calculated as a ratio of the PM/cytoplasm GFP signal based on mean gray values in narrow regions of the PM and next to it in the cytoplasm, avoiding vacuoles or nuclei.

Co-immunoprecipitation and western blot analysis

In vivo interactions within the exocyst subunits were detected by co-immunoprecipitation using the µMACS GFP-Tagged Protein Isolation Kit (Miltenyi Biotec) according to the manufacturer's instructions with only slight modification as described below. 0,6 g 10 d old *Arabidopsis* seedlings for each genotype were ground in liquid nitrogen and 1ml of Sec6/8 buffer was added (20 mM HEPES, pH 6.8, 150 mM NaCl, 1 mM EDTA, 1 mM DTT, 0.5% Tween-20, 100x protease inhibitor cocktail (Sigma-Aldrich)) instead of the provided Lysis buffers. Following the manufacturer's instructions the lysate was centrifuged at 10,000 × g for 10 min at 4°C. Anti-GFP magnetic beads (100 µL) were added to the supernatant and incubated on ice for 30 min. The solution was then transferred to a column attached to a magnetic stand and washed four times with 200 µL of Sec6/8 buffer, followed by one wash with 100 µL of washing buffer 2. Bound proteins were eluted with 100 µL of preheated elution buffer, separated by SDS–PAGE using 4–15% Mini-PROTEAN precast gels (Bio-Rad) and transferred to the membrane using the Trans-Blot Turbo Transfer System (Bio-Rad, Hercules, CA, USA). Membranes with bound proteins were blocked with blocking solution (1xPBS, 0,1% Tween, 5% skimmed milk) for 1h in RT and then washed three times for 10 min with washing solution (1xPBS, 0.1% Tween-20). The primary antibodies anti-Sec6 rabbit (oligopeptide generated antibody from Agrisera, dilution 1:10000) and anti-

GFP mouse (AS152987, Agrisera, dilution 1:1000) were incubated overnight at 4°C in the blocking solution. The three times of washing with washing solution was performed. Horseradish peroxidase-conjugated secondary antibodies (anti-rabbit 1:10000 and anti-mouse 1:10000; Promega) in blocking solution were applied for 1h in the RT. After the washing step the membrane was incubated with 1000 µL Amersham ECL Prime Western Blotting Detection Reagent (GE Healthcare, RPN2236) for 2 min and visualized using the ChemiDoc XRS+ Imaging system (Bio-Rad).

In silico structural analyses

Structural models of near full-length exocyst complexes from *Arabidopsis thaliana*, *Marchantia polymorpha*, *Klebsormidium nitens* and *Saccharomyces cerevisiae* were predicted using a local installation of the AlphaFold3 server (Abramson *et al.*, 2024). Prior to prediction, intrinsically disordered regions were removed from selected subunit sequences as follows: *Arabidopsis* SEC5a (residues 1–217 and 1043–1090) and SEC8 (1–34 and 226–307); *Marchantia* SEC5 (1–215 and 1042–1178) and SEC8 (1–8, 215–315, 397–440, and 539–610); *Klebsormidium* SEC5 (1–330, 1132–1155, and 1200–1346), SEC8 (207–310 and 536–636), SEC10 (1–106), SEC15 (1–32 and 767–825), and EXO84 (1–30); and *Saccharomyces* SEC3 (1–68 and 248–610), SEC5 (1–70), SEC8 (1–33 and 1011–1065), SEC10 (1–58 and 482–556), and SEC15 (1–61 and 767–910). The accuracy of structural predictions and the propensity for inter-chain interactions were assessed using the interaction prediction Score from Aligned Errors (ipSAE) metric (Dunbrack *et al.*, 2025). Structure visualization and residue contact analyses were performed using ChimeraX (Meng *et al.*, 2023).

ACKNOWLEDGMENTS

This work was supported by Charles University project GAUK 1544120 to S.H., by the Czech Science Foundation (GAČR) projects 22-28055S (to M.P.) and 23-05564S (to V.Ž.), and by the Ministry of Education, Youth and Sports (MEYS) project TowArds Next GENeration Crops, reg. no. CZ.02.01.01/00/22_008/0004581 of the ERDF Programme Johannes Amos Comenius. The Imaging Facility of the Institute of Experimental Botany CAS is supported by the MEYS CR (LM2023050 Czech-BioImaging), the Czech Academy of Sciences, and Institute of Experimental Botany CAS. Computational resources were provided by the e-INFRA CZ project (ID:90254), supported by the Ministry of Education, Youth and Sports of the Czech Republic. We thank Hana Soukupová, Lucie Brejšková and Jana Kaněrová for the technical assistance and Prof. Sabine Zachgo for the kind permission to use the *M. polymorpha* BoGa strain. Gratitude also goes to Prof. Takayuki Kohchi for making the pMpGWB101 plasmid available.

AUTHOR CONTRIBUTIONS

M.P., S.H., and V.Ž. designed the project. S.H. and E.J.D. performed most of the experiments. M.P. and V.Ž. supervised the study and contributed to the analyses and data interpretation. M.D., G.A.C., R.S., and P.P. contributed with material and data analyses. S.H., V.Ž., and M.P. wrote the article with input from all authors.

SUPPLEMENTARY DATA

The following materials are available in the online version of this article.

Supplemental Figure S1. Phylogenetic analyses of SEC3, SEC5, SEC6, SEC8, SEC10, SEC15, EXO70, and EXO84.

Supplemental Figure S2. Exon–intron architecture of EXO70 homologs from representative streptophyte lineages.

Supplemental Figure S3. Localization and overexpression analyses of Marchantia EXO70 paralogs in Marchantia gemmae.

Supplemental Figure S4. Localization, overexpression and complementation analyses of Klebsormidium and Marchantia EXO70 orthologs in Arabidopsis wild-type, *exo70A1*, *exo70B1* and *exo70H4* mutant backgrounds.

Supplemental Figure S5. Electrostatic potential clustering of EXO70 paralogs across streptophytes.

Supplemental Figure S6. Functional complementation, subcellular localization, and exocyst association of SEC3 orthologs in Arabidopsis wild-type, *sec3a* and *exo70A1* mutant backgrounds.

Supplemental Figure S7. The validation of AF3 comparative modelling approach and *in silico* structural analysis of plant exocyst complex variants.

Supplemental Figure S8. Comparative *in silico* structural analysis of native exocyst models and models lacking EXO70A1 subunit.

REFERENCES

Althoff F, Kopischke S, Zobell O, Ide K, Ishizaki K, Kohchi T, and Zachgo S. Comparison of the MpEF1α and CaMV35 promoters for application in *Marchantia polymorpha* overexpression studies. *Transgenic Research*. 2014:23:235–244. https://doi.org/10.1007/s11248-013-9746-z

Batystová K, Synek L, Klejchová M, Janková Drdová E, Sabol P, Potocký M, Žárský V, and Hála M. Diversification of SEC15a and SEC15b isoforms of an exocyst subunit in seed plants is manifested in their specific roles in *Arabidopsis* sporophyte and male gametophyte. *The Plant Journal*. 2022:110(5):1382–1396. https://doi.org/10.1111/tpj.15744

Bloch D, Pleskot R, Pejchar P, Potocký M, Trpkošová P, Cwiklik L, Vukašinović N, Sternberg H, Yalovsky S, and Žárský V. Exocyst SEC3 and phosphoinositides define sites of exocytosis in pollen tube initiation and growth. *Plant Physiology*. 2016:pp.00690.2016. https://doi.org/10.1104/pp.16.00690

Boehm C and Field MC. Evolution of late steps in exocytosis: conservation and specialization of the exocyst complex. *Wellcome Open Research*. 2019:4:112. https://doi.org/10.12688/wellcomeopenres.15142.2

Boyd C, Hughes T, Pypaert M, and Novick P. Vesicles carry most exocyst subunits to exocytic sites marked by the remaining two subunits, Sec3p and Exo70p. *Journal of Cell Biology*. 2004:167(5):889–901. https://doi.org/10.1083/jcb.200408124

Bowman JL, Arteaga-Vazquez M, Berger F, Briginshaw LN, Carella P, Aguilar-Cruz A, Davies KM, Dierschke T, Dolan L, Dorantes-Acosta AE, et al. The renaissance and enlightenment of Marchantia as a model system. *Plant Cell*. 2022:34(10):3512–3542. https://doi.org/10.1093/plcell/koac219

Cheng S, Xian W, Fu Y, Marin B, Keller J, Wu T, Sun W, Li X, Xu Y, Zhang Y, Wittek S, Reder T, Günther G, Gontcharov A, Wang S, Li L, Liu X, Wang J, Yang H, and Melkonian M. Genomes of subaerial Zygnematophyceae provide insights into land plant evolution. *Cell*. 2019:179(5):1057–1067.e14. https://doi.org/10.1016/j.cell.2019.10.019

Chong YT, Gidda SK, Sanford C, Parkinson J, Mullen RT, and Goring DR. Characterization of the *Arabidopsis thaliana* exocyst complex gene families by phylogenetic, expression profiling, and subcellular localization studies. *New Phytologist*. 2010:185(2):401–419. https://doi.org/10.1111/j.1469-8137.2009.03070.x

Clough SJ and Bent AF. Floral dip: a simplified method for *Agrobacterium*-mediated transformation of *Arabidopsis thaliana*. *The Plant Journal*. 1998:16(6):735–743. https://doi.org/10.1046/j.1365-313x.1998.00343.x

Cvrčková F, Grunt M, Bezvoda R, Hála M, Kulich I, Rawat A, and Žárský V. Evolution of the land plant exocyst complexes. *Frontiers in Plant Science*. 2012:3:159. https://doi.org/10.3389/fpls.2012.00159

De la Concepcion JC, Duverge H, Kim Y, Julian J, Xu HD, Watt MN, Ikene SA, Bianchi A, Grujic N, Papareddy RK, et al. Electrostatic changes enabled the diversification of an exocyst subunit via protein complex escape. *Nature Plants*. 2025:11(11):2350–2367. https://doi.org/10.1038/s41477-025-02135-1

Drdová EJ, Synek L, Pečenková T, Hála M, Kulich I, Fowler JE, Murphy AS, and Žárský V. The exocyst complex contributes to PIN auxin efflux carrier recycling and polar auxin transport in *Arabidopsis*. *The Plant Journal*. 2013:73(5):709–719. https://doi.org/10.1111/tpj.12074

Dunbrack RL. Rēs ipSAE loquunt: What's wrong with AlphaFold's ipTM score and how to fix it. *bioRxiv.* 2025:2025.02.10.637595. https://doi.org/10.1101/2025.02.10.637595

Edgar RC. MUSCLE: multiple sequence alignment with high accuracy and high throughput. *Nucleic Acids Research*. 2004:32(5):1792–1797. https://doi.org/10.1093/nar/gkh340

Elias M. The exocyst complex in plants. *Cell Biology International*. 2003:27(3):199–201. https://doi.org/10.1016/S1065-6995(02)00349-9

Fendrych M, Synek L, Pečenková T, Drdová EJ, Sekereš J, de Rycke R, Nowack MK, and Žárský V. Visualization of the exocyst complex dynamics at the plasma membrane of *Arabidopsis thaliana*. *Molecular Biology of the Cell*. 2013:24(4):510–520. https://doi.org/10.1091/mbc.e12-06-0492

Fendrych M, Synek L, Pečenková T, Toupalová H, Cole R, Drdová E, Nebesářová J, Šedinová M, Hála M, Fowler JE, and Žárský V. The *Arabidopsis* exocyst complex is involved in cytokinesis and cell plate maturation. T*he Plant Cell.* 2010:22(9):3053–3065. https://doi.org/10.1105/tpc.110.074351

Gamborg OL, Miller RA, and Ojima K. Nutrient requirements of suspension cultures of soybean root cells. *Experimental Cell Researc*h. 1968:50(1):151–158. https://doi.org/10.1016/0014-4827(68)90403-5

Gouy M, Guindon S, and Gascuel O. SeaView version 4: a multiplatform graphical user interface for sequence alignment and phylogenetic tree building. *Molecular Biology and Evolution*. 2010:27(2):221–224. https://doi.org/10.1093/molbev/msp259

Guindon S, Dufayard J-F, Lefort V, Anisimova M, Hordijk W, and Gascuel O. New Algorithms and Methods to Estimate Maximum-Likelihood Phylogenies: Assessing the Performance of PhyML 3.0. *Systematic Biol*ogy 2010:59(3):307–321. https://doi.org/10.1093/sysbio/syq010

Hála M, Cole R, Synek L, Drdová E, Pečenková T, Nordheim A, Lamkemeyer T, Madlung J, Hochholdinger F, Fowler JE, and Žárský V. An exocyst complex functions in plant cell

growth in *Arabidopsis* and tobacco. *The Plant Cell.* 2008:20(5):1330–1345. https://doi.org/10.1105/tpc.108.059105

He B and Guo W. The exocyst complex in polarized exocytosis. *Current Opinion in Cell Biology.* 2009:21(4):537–542. https://doi.org/10.1016/j.ceb.2009.04.007

He B, Xi F, Zhang X, Zhang J, and Guo W. Exo70 interacts with phospholipids and mediates the targeting of the exocyst to the plasma membrane. *The EMBO Journal.* 2007:26(18):4053–4065. https://doi.org/10.1038/sj.emboj.7601834

Heider MR, Gu M, Duffy CM, Mirza AM, Marcotte LL, Walls AC, Farrall N, Hakhverdyan Z, Field MC, Rout MP, Frost A, and Munson M. Subunit connectivity, assembly determinants and architecture of the yeast exocyst complex. *Nature Structural & Molecular Biology.* 2016:23(1):59–66. https://doi.org/10.1038/nsmb.3146

Heider MR and Munson M. Exorcising the exocyst complex. *Traffic*. 2012:13(7):898–907. https://doi.org/10.1111/j.1600-0854.2012.01353.x

Irastorza-Azcarate I, Castaño-Díez D, Devos DP, and Gallego O. Live-cell structural biology to solve biological mechanisms: the case of the exocyst. *Structure*. 2019:27(6):886–892. https://doi.org/10.1016/j.str.2019.04.010

Janková Drdová E, Klejchová M, Janko K, Hála M, Soukupová H, Cvrčková F, and Žárský V. Developmental plasticity of *Arabidopsis* hypocotyl is dependent on exocyst complex function. *Journal of Experimental Botany*. 2019:70(4):1255–1265. https://doi.org/10.1093/jxb/erz005

Jiao C, Sørensen I, Sun X, Sun H, Behar H, Alseekh S, Philippe G, Lopez KP, Sun LI, Reed R, and Jeon S. The Penium margaritaceum genome: hallmarks of the origins of land plants. *Cell*. 2020:181(5):1097–1111. https://doi.org/10.1016/j.cell.2020.04.019

Katoh K and Standley DM. MAFFT Multiple Sequence Alignment Software Version 7: Improvements in Performance and Usability. *Molecular Biology and Evolution*. 2013:30(4):772–780. https://doi.org/10.1093/molbev/mst010

Koumandou VL, Dacks JB, Coulson RM, and Field MC. Control systems for membrane fusion in the ancestral eukaryote; evolution of tethering complexes and SM proteins. *BMC Evolutionary Biology.* 2007:7(1):29. https://doi.org/10.1186/1471-2148-7-29

Kulich I, Pečenková T, Sekereš J, Smetana O, Fendrych M, Foissner I, Höftberger M, and Žárský V. Arabidopsis exocyst subcomplex containing subunit EXO70B1 is involved in autophagy-related transport to the vacuole. *Traffic*. 2013:14(11):1155–1165. https://doi.org/10.1111/tra.12101

Kulich I, Cole R, Drdová E, Cvrčková F, Soukup A, Fowler J, and Žárský V. Arabidopsis exocyst subunits SEC8 and EXO70A1 and exocyst interactor ROH1 are involved in the localized deposition of seed coat pectin. *New Phytologist*. 2010:188(2):615–625. https://doi.org/10.1111/j.1469-8137.2010.03372.x

Kulich I, Vojtíková Z, Glanc M, Ortmannová J, Rasmann S, and Žárský V. Cell wall maturation of Arabidopsis trichomes is dependent on exocyst subunit EXO70H4 and involves callose deposition. *Plant Physiology.* 2015:168(1):120–131. https://doi.org/10.1104/pp.15.00112

Kulich I, Vojtíková Z, Sabol P, Ortmannová J, Neděla V, Tihlaříková E, and Žárský V. Exocyst subunit EXO70H4 has a specific role in callose synthase secretion and silica accumulation. *Plant Physiology.* 2018:176(3):2040–2051. https://doi.org/10.1104/pp.17.01693

Kumari R, Nath T, Pflaum J, R I, Vinay S, Wilfling F, and Manjithaya R. The autophagy-specific exocyst subcomplex contributes to phagophore assembly site integrity by promoting phagophore expansion. *Proceedings of the National Academy of Sciences*. 2025:122(41):e2426476122. https://doi.org/10.1073/pnas.2426476122

Lepore DM, Martínez-Núñez L, and Munson M. Exposing the elusive exocyst structure. *Trends in Biochemical Sciences.* 2018:43(9):714–725. https://doi.org/10.1016/j.tibs.2018.06.012

Li F-W, Nishiyama T, Waller M, Frangedakis E, Keller J, Li Z, Fernandez-Pozo N, Barker MS, Bennett T, Blázquez MA, Cheng S, Cuming AC, de Vries J, de Vries S, Delaux P-M, Diop IS, Harrison CJ, Hauser D, Hernández-García J, and Szövényi P. Anthoceros genomes illuminate the origin of land plants and the unique biology of hornworts. *Nature Plants.* 2020:6(3):259–272. https://doi.org/10.1038/s41477-020-0618-2

Liu D, Li X, Shen D, and Novick P. Two subunits of the exocyst, Sec3p and Exo70p, can function exclusively on the plasma membrane. *Molecular Biology of the Cell*. 2018:29(6):736–750. https://doi.org/10.1091/mbc.E17-08-0518

Luo G, Zhang J, and Guo W. The role of Sec3p in secretory vesicle targeting and exocyst complex assembly. *Molecular Biology of the Cell*. 2014:25(23):3813–3822. https://doi.org/10.1091/mbc.e14-04-0907

Maib H and Murray DH. A mechanism for exocyst-mediated tethering via Arf6 and PIP5K1C-driven phosphoinositide conversion. *Current Biology*. 2022:32(13):2821–2833.e6. https://doi.org/10.1016/j.cub.2022.04.089

Marković V, Kulich I, and Žárský V. Functional specialization within the EXO70 gene family in Arabidopsis. *International Journal of Molecular Sciences*. 2021:22(14):7595. https://doi.org/10.3390/ijms22147595

Mei K, Li Y, Wang S, Shao G, Wang J, Ding Y, Luo G, Yue P, Liu J-J, Wang X, Dong M-Q, Wang H-W, and Guo W. Cryo-EM structure of the exocyst complex. *Nature Structural & Molecular Biology.* 2018:25(2):139–146. https://doi.org/10.1038/s41594-017-0016-2

Munson M and Novick P. The exocyst defrocked, a framework of rods revealed. *Nature Structural & Molecular Biology*. 2006:13(7):577–581. https://doi.org/10.1038/nsmb1097

Nishida-Fukuda H. The Exocyst: Dynamic Machine or Static Tethering Complex? *BioEssays*. 2019:41(8):1900056. https://doi.org/10.1002/bies.201900056

Nishiyama T, Sakayama H, de Vries J, Buschmann H, Saint-Marcoux D, Ullrich KK, Haas FB, Vanderstraeten L, Becker D, Lang D, Vosolsobě S, Rombauts S, Wilhelmsson PKI, Janitza P, Kern R, Heyl A, Rümpler F, Villalobos LIA C, Clay JM, and Rensing SA. The Chara genome: secondary complexity and implications for plant terrestrialization. *Cell*. 2018a:174(2):448–464.e24. https://doi.org/10.1016/j.cell.2018.06.033

Pečenková T, Hála M, Kulich I, Kocourková D, Drdová E, Fendrych M, Toupalová H, and Žárský V. The role for the exocyst complex subunits Exo70B2 and Exo70H1 in the plant–pathogen interaction. *Journal of Experimental Botany*. 2011:62(6):2107–2116. https://doi.org/10.1093/jxb/erq402

Pleskot R, Cwiklik L, Jungwirth P, Žárský V, and Potocký M. Membrane targeting of the yeast exocyst complex. *Biochimica et Biophysica Acta - Biomembranes.* 2015:1848(7):1481–1489. https://doi.org/10.1016/j.bbamem.2015.03.026

Rawat A, Brejšková L, Hála M, Cvrčková F, and Žárský V. The Physcomitrella patens exocyst subunit EXO70.3d has distinct roles in growth and development, and is essential for completion of the moss life cycle. *New Phytologist.* 2017:216(2):438–454. https://doi.org/10.1111/nph.14548

Rensing SA. How plants conquered land. *Cell*. 2020:181(5):964–966. https://doi.org/10.1016/j.cell.2020.05.011

Richter S, Wenzel A, Stein M, Gabdoulline RR, and Wade RC. webPIPSA: a web server for the comparison of protein interaction properties. *Nucleic Acids Research*. 2008:36(suppl_2):W276–W280. https://doi.org/10.1093/nar/gkn181

Schekman R and Novick P. 23 genes, 23 years later. *Cell*. 2004:116:S13–S15. https://doi.org/10.1016/S0092-8674(03)00972-3

Schindelin J, Arganda-Carreras I, Frise E, Kaynig V, Longair M, Pietzsch T, Preibisch S, Rueden C, Saalfeld S, Schmid B, et al. Fiji: an open-source platform for biological-image analysis. *Nature Methods*. 2012:9(7):676–682. https://doi.org/10.1038/nmeth.2019

Sekereš J, Pleskot R, Pejchar P, Žárský V, and Potocký M. The song of lipids and proteins: dynamic lipid-protein interfaces in the regulation of plant cell polarity at different scales. *Journal of Experimental Botany*. 2015:66(6):1587–1598. https://doi.org/10.1093/jxb/erv052

Solovyev V, Kosarev P, Seledsov I, and Vorobyev D. Automatic annotation of eukaryotic genes, pseudogenes and promoters. *Genome Biology*. 2006:7(1):S10. https://doi.org/10.1186/gb-2006-7-s1-s10

Su D, Yang L, Shi X, Ma X, Zhou X, Hedges SB, and Zhong B. Large-scale phylogenomic analyses reveal the monophyly of bryophytes and Neoproterozoic origin of land plants. *Molecular Biology and Evolution*. 2021:38(8):3332–3344. https://doi.org/10.1093/molbev/msab106

Synek L, Pleskot R, Sekereš J, Serrano N, Vukašinović N, Ortmannová J, Klejchová M, Pejchar P, Batystová K, Gutkowska M, Janková-Drdová E, Marković V, Pečenková T, Šantrůček J, Žárský V, and Potocký M. Plasma membrane phospholipid signature recruits the plant exocyst complex via the EXO70A1 subunit. *Proceedings of the National Academy of Sciences.* 2021:118(36):e2105287118. https://doi.org/10.1073/pnas.2105287118

Synek L, Schlager N, Eliáš M, Quentin M, Hauser M-T, and Žárský V. AtEXO70A1, a member of a family of putative exocyst subunits specifically expanded in land plants, is important for polar growth and plant development. *The Plant Journal*. 2006:48(1):54–72. https://doi.org/10.1111/j.1365-313X.2006.02854.x

TerBush DR, Maurice T, Roth D, and Novick P. The exocyst is a multiprotein complex required for exocytosis in Saccharomyces cerevisiae. *The EMBO Journal.* 1996:15(23):6483–6494. https://doi.org/10.1002/j.1460-2075.1996.tb01039.x

Tsuboyama S and Kodama Y. AgarTrap protocols on your benchtop: simple methods for Agrobacterium-mediated genetic transformation of the liverwort Marchantia polymorpha. *Plant Biotechnology*. 2018:35(2):93–99. https://doi.org/10.5511/plantbiotechnology.18.0312b

van Gisbergen PAC, Wu S-Z, Chang M, Pattavina KA, Bartlett ME, and Bezanilla M. An ancient Sec10–formin fusion provides insights into actin-mediated regulation of exocytosis. *Journal of Cell Biology.* 2018:217(3):945–957. https://doi.org/10.1083/jcb.201705084

Vukašinović N, Oda Y, Pejchar P, Synek L, Pečenková T, Rawat A, Sekereš J, Potocký M, and Žárský V. Microtubule-dependent targeting of the exocyst complex is necessary for xylem development in Arabidopsis. *New Phytologist.* 2017:213(3):1052–1067. https://doi.org/10.1111/nph.14267

Wang S, Li L, Li H, Sahu SK, Wang H, Xu Y, Xian W, Song B, Liang H, Cheng S, Chang Y, Song Y, Çebi Z, Wittek S, Reder T, Peterson M, Yang H, Wang J, Melkonian B, and Liu X. Genomes of early-diverging streptophyte algae shed light on plant terrestrialization. *Nature Plants*. 2019:6(2):95–106. https://doi.org/10.1038/s41477-019-0560-3

Wickell D, Kuo L-Y, Yang H-P, Dhabalia Ashok A, Irisarri I, Dadras A, de Vries S, de Vries J, Huang Y-M, Li Z, Barker MS, Hartwick NT, Michael TP, and Li F-W. Underwater CAM photosynthesis elucidated by Isoetes genome. *Nature Communications.* 2021:12(1):6348. https://doi.org/10.1038/s41467-021-26644-7

Wu H, Rossi G, and Brennwald P. The ghost in the machine: small GTPases as spatial regulators of exocytosis. *Trends in Cell Biology.* 2008:18(9):397–404. https://doi.org/10.1016/j.tcb.2008.06.007

Yue P, Zhang Y, Mei K, Wang S, Lesigang J, Zhu Y, Dong G, and Guo W. Sec3 promotes the initial binary t-SNARE complex assembly and membrane fusion. *Nature Communications.* 2017:8(1):14236. https://doi.org/10.1038/ncomms14236

Žárský V. Exocyst functions in plants: secretion and autophagy. *FEBS Letters.* 2022:596(17):2324–2334. https://doi.org/10.1002/1873-3468.14430

Žárský V, Kulich I, Fendrych M, and Pečenková T. Exocyst complexes multiple functions in plant cells secretory pathways. *Current Opinion in Plant Biology.* 2013:16(6):726–733. https://doi.org/10.1016/j.pbi.2013.10.013

Žárský V, Sekereš J, Kubátová Z, Pečenková T, and Cvrčková F. Three subfamilies of exocyst EXO70 family subunits in land plants: early divergence and ongoing functional specialization. *J Exp Bot*. 2020:71(1):49–62. https://doi.org/10.1093/jxb/erz423

Zhang X, Orlando K, He B, Xi F, Zhang J, Zajac A, and Guo W. Membrane association and functional regulation of Sec3 by phospholipids and Cdc42. Journal of Cell Biology. 2008:180(1):145–158. https://doi.org/10.1083/jcb.200704128

Zhang C, Shine M, Pyle AM, and Zhang Y. US-align: universal structure alignments of proteins, nucleic acids, and macromolecular complexes. *Nature Methods*. 2022:19(9):1109–1115. https://doi.org/10.1038/s41592-022-01585-1

Zhao Y, Liu J, Yang C, Capraro BR, Baumgart T, Bradley RP, Ramakrishnan N, Xu X, Radhakrishnan R, Svitkina T, and Guo W. Exo70 generates membrane curvature for morphogenesis and cell migration. *Developmental Cell*. 2013:26(3):266–278. https://doi.org/10.1016/j.devcel.2013.07.007

Zhou H-X and Pang X. Electrostatic Interactions in Protein Structure, Folding, Binding, and Condensation. *Chem Rev*. 2018:118(4):1691–1741. https://doi.org/10.1021/acs.chemrev.7b00305

Zhu J, Li M, Zhao M, Luo Y, Ren M, Zhao K, Xu J, Wu Y, Liu Y, Wu Z, et al. OsSEC3A, a key exocyst subunit, is required for the emergence of crown root in rice. *New Phytologist*. 2026:249(2):917–929. https://doi.org/10.1111/nph.70696